

**PREDICTION OF WEB WRINKLING INDUCED BY
ROLLER DEFLECTION**

By

PEDRO J. ARIAS

Bachelor of Engineering

Universidad Central de Venezuela

Caracas, Venezuela

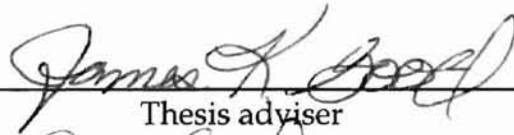
1981

Submitted to the Faculty of the
Graduate College of the
Oklahoma State University
in partial fulfillment of
the requirements for
the Degree of
MASTER OF SCIENCE
July, 1998

OKLAHOMA STATE UNIVERSITY

PREDICTION OF WEB WRINKLING INDUCED BY
ROLLER DEFLECTION

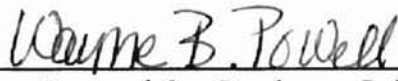
Thesis Approved:



Thesis adviser







Dean of the Graduate College

ACKNOWLEDGMENTS

I would like to thank my adviser, Dr. J. K. Good for his guidance, support and patience during my graduate studies and in the course of this research work. I would also like to thank to Dr. C. E. Price and Dr. H. B. Lu for serving in my committee.

I would like to extend many thanks the school of Mechanical and Aerospace Engineering and the Web Handling Research Center for the research assistantship given to me during this research and those fellows who provided suggestions and help: Ronald Markum, Pat Straughn and Carrie Reynolds.

I specially thank and love my wife Licelot for her support and taking care of our children since I have returned to school, and my parents and family for their constant encouragement and moral support during my graduate studies.

TABLE OF CONTENTS

	Page
CHAPTER 1: INTRODUCTION.....	13
CHAPTER 2: THEORETICAL ANALYSIS.....	17
2.1 TRACTION BOUNDARY VALUED PROBLEM FOR A WEB SPAN.....	18
2.2 BEAM THEORY TO PREDICT ROLLER DEFLECTION DUE TO A WEB TENSION.....	25
2.3 THEORY OF LATERAL COMPRESSION CAUSED BY ROLLER DEFLECTION.....	31
2.4 MINIMUM PARABOLIC TRACTION THAT CAUSES WEB WRINKLING DUE TO ROLLER CURVATURE.....	35
CHAPTER 3: EXPERIMENTAL SETUP AND PROCEDURE.....	40
3.1 TESTING MACHINE.....	40
3.2 WEB PROPERTIES AND DIMENSIONS.....	43
3.3 ROLLER PROPERTIES AND DIMENSIONS.....	44
3.4 EXPERIMENTAL PROCEDURE.....	45
3.5 WEB AND ROLLER SURFACE ROUGHNESS.....	46
3.6 COEFFICIENT OF FRICTION BETWEEN WEB AND ROLLER.....	47
CHAPTER 4: EXPERIMENTAL RESULTS.....	48
4.1 EXPERIMENTAL WRINKLING CONDITIONS.....	48
4.2 EXPERIMENTAL WEB AND ROLLER ROUGHNESS.....	55
4.3 COEFFICIENT OF FRICTION BETWEEN WEB AND ROLLER.....	56
CHAPTER 5: ANALYSIS OF EXPERIMENTAL DATA.....	57
5.1 INITIAL THEORETICAL COMPUTATIONS.....	57
5.2 COMPARISON BETWEEN EXPERIMENTAL RESULTS AND INITIAL THEORETICAL COMPUTATIONS.....	60
5.3 MODIFIED STRESS WRINKLING CONDITION.....	76
CHAPTER 6: CONCLUSIONS AND RECOMMENDATIONS.....	88
REFERENCES.....	90

LIST OF FIGURES

Figure	Page
1. WEB SPAN MODELED AS A THIN PLATE.....	18
2. A ROLLER SUBJECTED TO A PARABOLIC WEB TENSION f MODELED AS A SIMPLY SUPPORTED BEAM....	26
3. FORCES ACTING OVER A ROLLER DUE TO WEB TENSION.....	27
4. TEST SECTION.....	28
5. SCHEMATIC OF AN ELEMENTAL WEB PIECE AT THE CONTACT LINE WEB-ROLLER.....	32
6. SCHEMATIC OF AN ELEMENTAL PARABOLIC WEB TRACTION d_y APPLIED ON AN ELEMENTAL WEB WIDTH.....	35
7. IMAGINARY POINTS ALONG THE CONTACT LINE WEB-ROLLER.....	36
8. TESTING MACHINE IN THE WHRC AT OSU.....	40
9. TESTING MACHINE IN THE WHRC AT OSU.....	41
10. TESTING MACHINE IN THE WHRC AT OSU.....	41
11. GENERAL LAYOUT OF THE WEB LINE ON THE TESTING MACHINE.....	42
12. 31.75MM (1 ½ IN.) ROLLER ASSEMBLED WITH THE TWO MICROMETERS ON THE TESTING MACHINE..	45
13. TROUGHS OR WRINKLES AT THE WEB SPAN BEFORE WRINKLING FORMATION IN THE WEB WRAPPING THE ROLLER.....	49
14. INITIAL WRINKLING FORMATION AT THE ROLLER CENTER.....	50
15. WEB WRINKLING OVER THE ROLLER.....	50
16. INITIAL WRINKLING FORMATION ON THE 38.10 MM (1 ½ IN.) ROLLER.....	51
17. WEB WRINKLING OVER THE 38.10 MM (1 ½ IN.) ROLLER.....	51
18. WEB WRINKLING OVER THE 50.8 MM (2 IN.) ROLLER.....	52
19. THEORETICAL STRESS WRINKLING CONDITION.....	58
20. THEORETICAL COMPATIBILITY WRINKLING CONDITION.....	59
21. THEORETICAL FRICTIONAL WRINKLING.....	59
22. MINIMUM THEORETICAL LOAD R_w theor. ACCORDING TO INITIAL CALCULATIONS VS. EXPERIMENTAL LOADS R_w exp. FOR 31.75MM (1 ¼ IN.) ROLLER, POLYESTER GAUGE 48, SPAN = 381 MM AT 14, 29, 42 M/MIN.....	61
23. MINIMUM THEORETICAL LOAD R_w theor. ACCORDING TO INITIAL CALCULATIONS VS. EXPERIMENTAL LOADS R_w exp. FOR 31.75MM (1 ¼ IN.) ROLLER, POLYESTER GAUGE 48, SPAN = 508 MM AT 13, 29 AND 41 M/MIN.....	62
24. MINIMUM THEORETICAL LOAD R_w theor. ACCORDING TO INITIAL CALCULATIONS VS. EXPERIMENTAL LOADS R_w exp. FOR 38.10 MM (1 ½ IN.) ROLLER, POLYESTER GAUGE 92, SPAN = 381 MM AT 14, 27 AND 41 M/MIN.....	62

25. MINIMUM THEORETICAL LOAD R_w theor. ACCORDING TO INITIAL CALCULATIONS VS. EXPERIMENTAL LOADS R_w exp. FOR 38.10 MM (1 1/2 IN.) ROLLER, POLYESTER GAUGE 92, SPAN = 508 MM AT 13, 28 AND 41 M/MIN.....	63
26. MINIMUM THEORETICAL LOAD R_w theor. ACCORDING TO INITIAL CALCULATIONS VS. EXPERIMENTAL LOADS R_w exp. FOR 38.10 MM (1 1/2 IN.) ROLLER, POLYESTER GAUGE 142, SPAN = 381 MM AT 13, 30 AND 40 M/MIN.....	63
27. MINIMUM THEORETICAL LOAD R_w theor. ACCORDING TO INITIAL CALCULATIONS VS. EXPERIMENTAL LOADS R_w exp. FOR 38.10 MM (1 1/2 IN.) ROLLER, POLYESTER GAUGE 142, SPAN = 508 MM AT 12, 30 AND 39 M/MIN	64
28. THEORETICAL ROLLER CENTER DEFLECTION $u_{r-theor}$. ACCORDING TO INITIAL COMPUTATIONS VS. EXPERIMENTAL RELATIVE DEFLECTIONS u_{r-exp} . FOR 31.75 MM (1 1/4 IN.) ROLLER, POLYESTER GAUGE 48, SPAN = 381 MM AT 14, 29 AND 42 M/MIN.....	65
29. THEORETICAL ROLLER CENTER DEFLECTION $u_{r-theor}$. ACCORDING TO INITIAL COMPUTATIONS VS. EXPERIMENTAL RELATIVE DEFLECTIONS u_{r-exp} FOR 31.75 MM (1 1/4 IN.) ROLLER, POLYESTER GAUGE 48, SPAN = 508 MM AT 13, 29 AND 40 M/MIN.....	65
30. THEORETICAL ROLLER CENTER DEFLECTION $u_{r-theor}$ ACCORDING TO INITIAL COMPUTATIONS VS. EXPERIMENTAL RELATIVE DEFLECTIONS u_{r-exp} . FOR 38.10 MM (1 1/2 IN.) ROLLER, POLYESTER GAUGE 92, SPAN = 381 MM AT 14, 27 AND 41 M/MIN.....	66
31. THEORETICAL ROLLER CENTER DEFLECTION $u_{r-theor}$ ACCORDING TO INITIAL COMPUTATIONS VS. EXPERIMENTAL RELATIVE DEFLECTION u_{r-exp} FOR 38.10 MM (1 1/2 IN.) ROLLER, POLYESTER GAUGE 92, SPAN = 508 MM AT 13, 28 AND 41 M/MIN.....	66
32. THEORETICAL ROLLER CENTER DEFLECTION $u_{r-theor}$. ACCORDING TO INITIAL COMPUTATIONS VS. EXPERIMENTAL RELATIVE DEFLECTIONS u_{r-exp} . FOR 38.10 MM (1 1/2 IN.) ROLLER, POLYESTER GAUGE 142, SPAN = 381 MM AT 13, 30 AND 40 M/MIN	67
33. THEORETICAL ROLLER CENTER DEFLECTION $u_{r-theor}$. ACCORDING TO INITIAL COMPUTATIONS VS. EXPERIMENTAL RELATIVE DEFLECTIONS u_{r-exp} FOR 38.10 MM (1 1/2 IN.) ROLLER, POLYESTER GAUGE 142, SPAN = 508 MM AT 12, 30 AND 39 M/MIN.....	67
34. THEORETICAL INTERNAL STRESS IN CMD σ_y VS. CRITICAL BUCKLING STRESS σ_{cr} AT EXPERIMENTAL NET FORCES R_w exp. FOR 31.75 MM (1 1/4 IN.) ROLLER, POLYESTER GAUGE 48 AND SPAN = 381 MM.....	69
35. THEORETICAL INTERNAL STRESS IN CMD σ_y VS. CRITICAL BUCKLING STRESS σ_{cr} AT EXPERIMENTAL NET FORCES R_w exp. FOR 31.75 MM (1 1/4 IN.) ROLLER, POLYESTER GAUGE 48 AND SPAN= 508 MM.....	70
36. THEORETICAL INTERNAL STRESS IN CMD σ_y VS. CRITICAL BUCKLING STRESS σ_{cr} AT EXPERIMENTAL NET FORCES R_w exp. FOR 38.10 MM (1 1/2 IN.) ROLLER, POLYESTER GAUGE 92 AND SPAN = 381 MM.....	70
37. THEORETICAL INTERNAL STRESS IN CMD σ_y VS. CRITICAL BUCKLING STRESS σ_{cr} AT EXPERIMENTAL NET FORCES R_w exp. FOR 38.10 MM (1 1/2 IN.) ROLLER, POLYESTER GAUGE 92 AND SPAN = 508 MM.....	71

38. THEORETICAL INTERNAL STRESS IN CMD σ_y VS. CRITICAL BUCKLING STRESS σ_{cr} AT EXPERIMENTAL NET FORCES $R_w \text{ exp.}$ FOR 38.10 MM (1 ½ IN.) ROLLER, POLYESTER GAUGE 142 AND SPAN = 381 MM.....	71
39. THEORETICAL INTERNAL STRESS IN CMD σ_y VS. CRITICAL BUCKLING STRESS σ_{cr} AT EXPERIMENTAL NET FORCES $R_w \text{ exp.}$ FOR 38.10 MM (1 ½ IN.) ROLLER, POLYESTER GAUGE 142 AND SPAN = 508 MM.....	72
40. THEORETICAL ($u_r \text{ theor.}$) VS. EXPERIMENTAL ($u_r \text{ exp.}$) ROLLER CENTER DEFLECTIONS AT EXPERIMENTAL LOADS $R_w \text{ exp.}$ FOR 31.75 MM (1 ¼ IN.) ROLLER, POLYESTER GAUGE 48 AND SPAN = 381 MM AT 14, 29 AND 42 M/MIN.....	73
41. THEORETICAL ($u_r \text{ theor.}$) VS. EXPERIMENTAL ($u_r \text{ exp.}$) ROLLER CENTER DEFLECTIONS AT EXPERIMENTAL LOADS $R_w \text{ exp.}$ FOR 31.75 MM (1 ¼ IN.) ROLLER, POLYESTER GAUGE 48 AND SPAN = 508 MM AT 13, 29 AND 41 M/MIN.....	73
42. THEORETICAL ($u_r \text{ theor.}$) VS. EXPERIMENTAL ($u_r \text{ exp.}$) ROLLER CENTER DEFLECTIONS AT EXPERIMENTAL LOADS $R_w \text{ exp.}$ FOR 38.10 MM (1 ½ IN.) ROLLER, POLYESTER GAUGE 92 AND SPAN = 381 MM AT 14, 27 AND 41M/MIN.....	74
43. THEORETICAL ($u_r \text{ theor.}$) VS. EXPERIMENTAL ($u_r \text{ exp.}$) ROLLER CENTER DEFLECTIONS AT EXPERIMENTAL LOADS $R_w \text{ exp.}$ FOR 38.10 MM (1 ½ IN.) ROLLER, POLYESTER GAUGE 92 AND SPAN = 508 MM AT 13, 28 AND 41M/MIN.....	74
44. THEORETICAL ($u_r \text{ theor.}$) VS. EXPERIMENTAL ($u_r \text{ exp.}$) ROLLER CENTER DEFLECTIONS AT EXPERIMENTAL LOADS $R_w \text{ exp.}$ FOR 38.10MM (1 ½ IN.) ROLLER, POLYESTER GAUGE 142 AND SPAN = 381 MM AT 13, 30 AND 40 M/MIN.....	75
45. THEORETICAL ($u_r \text{ theor.}$) VS. EXPERIMENTAL ($u_r \text{ exp.}$) ROLLER CENTER DEFLECTIONS AT EXPERIMENTAL LOADS $R_w \text{ exp.}$ FOR 38.10 MM (1 ½ IN.) ROLLER, POLYESTER GAUGE 142 AND SPAN = 508 MM AT 12, 30 AND 39 M/MIN.....	75
46. MINIMUM THEORETICAL LOAD $R_w \text{ theor.}$ CONSIDERING TOTAL STRESS IN CMD σ_{ly} VS. EXPERIMENTAL LOADS $R_w \text{ exp.}$ FOR 31.75 MM (1 ¼ IN.) ROLLER, POLYESTER GAUGE 48, SPAN = 381 MM AT 14, 29 AND 42 M/MIN.....	78
47. MINIMUM THEORETICAL LOAD $R_w \text{ theor.}$ CONSIDERING TOTAL STRESS IN CMD σ_{ly} VS. EXPERIMENTAL LOADS $R_w \text{ exp.}$ FOR 31.75 MM (1 ¼ IN.) ROLLER, POLYESTER GAUGE 48, SPAN = 508 MM AT 13, 29 AND 41 M/MIN.....	79
48. MINIMUM THEORETICAL LOAD $R_w \text{ theor.}$ CONSIDERING TOTAL STRESS IN CMD σ_{ly} VS. EXPERIMENTAL LOADS $R_w \text{ exp.}$ FOR 38.10 MM (1 ½ IN.) ROLLER, POLYESTER GAUGE 92, SPAN = 381MM AT 14, 27 AND 41 M/MIN.	79
49. MINIMUM THEORETICAL LOAD $R_w \text{ theor.}$ CONSIDERING TOTAL STRESS IN CMD σ_{ly} VS. EXPERIMENTAL LOADS $R_w \text{ exp.}$ FOR 38.10 MM (1 ½ IN.) ROLLER, POLYESTER GAUGE 92, SPAN = 508 MM AT 13, 28 AND 41 M/MIN.....	80

50. MINIMUM THEORETICAL LOAD R_w theor. CONSIDERING TOTAL STRESS IN CMD σ_{ty} VS. EXPERIMENTAL LOADS R_w exp. FOR 38.10 MM (1 ½ IN.) ROLLER, POLYESTER GAUGE 142, SPAN = 381 MM AT 13, 30 AND 40 M/MIN.....	80
51. MINIMUM THEORETICAL LOAD R_w theor. CONSIDERING TOTAL STRESS IN CMD σ_{ty} VS. EXPERIMENTAL LOADS R_w exp. FOR 38.10 MM (1 ½ IN.) ROLLER, POLYESTER GAUGE 142, SPAN = 508 MM AT 12, 30 AND 39 M/MIN.....	81
52. THEORETICAL (u_r theor.) VS. EXPERIMENTAL (u_r exp.) ROLLER CENTER DEFLECTIONS CONSIDERING TOTAL STRESS IN CMD σ_{ty} FOR 31.75 MM (1 ¼ IN.) ROLLER, POLYESTER GAUGE 48 AND SPAN = 381 MM AT 14, 29 AND 42 M/MIN.	81
53. THEORETICAL (u_r theor.) VS. EXPERIMENTAL (u_r exp.) ROLLER CENTER DEFLECTIONS CONSIDERING TOTAL STRESS IN CMD σ_{ty} FOR 31.75 MM (1 ¼ IN.) ROLLER, POLYESTER GAUGE 48 AND SPAN = 508 MM AT 13, 29 AND 41 M/MIN.	82
54. THEORETICAL (u_r theor.) VS. EXPERIMENTAL (u_r exp.) ROLLER CENTER DEFLECTIONS CONSIDERING TOTAL STRESS IN CMD σ_{ty} FOR 38.10 MM (1 ½ IN.) ROLLER, POLYESTER GAUGE 92 AND SPAN = 381 MM AT 14, 27 AND 41 M/MIN.	82
55. THEORETICAL (u_r theor.) VS. EXPERIMENTAL (u_r exp.) ROLLER CENTER DEFLECTIONS CONSIDERING TOTAL STRESS IN CMD σ_{ty} FOR 38.10 MM (1 ½ IN.) ROLLER, POLYESTER GAUGE 92 AND SPAN = 508 MM AT 13, 28 AND 41 M/MIN.	83
56. THEORETICAL (u_r theor.) VS. EXPERIMENTAL (u_r exp.) ROLLER CENTER DEFLECTIONS CONSIDERING TOTAL STRESS IN CMD σ_{ty} FOR 38.10 MM (1 ½ IN.) ROLLER, POLYESTER GAUGE 142 AND SPAN =381 MM AT 13, 30 AND 40 M/MIN.	83
57. THEORETICAL (u_r theor.) VS. EXPERIMENTAL (u_r exp.) ROLLER CENTER DEFLECTIONS CONSIDERING TOTAL STRESS IN CMD σ_{ty} FOR 38.10 MM (1 ½ IN.) ROLLER, POLYESTER GAUGE 142 AND SPAN = 508 MM AT 12, 30 AND 39 M/MIN.	84
58. L.ATERAL SURFACE FORCE f_u VS. INTERNAL FORCE f_i CONSIDERING σ_{ty} FOR 31.75 MM (1 ¼ IN.) ROLLER AND POLYESTER GAUGE 48 AT THE TESTED VELOCITIES.....	86
59. LATERAL SURFACE FORCE f_u VS. INTERNAL FORCE f_i CONSIDERING σ_{ty} FOR 38.10 MM (1 ½ IN.) ROLLER AND POLYESTER GAUGE 92 AT THE TESTED VELOCITIES.....	87
60. LATERAL SURFACE FORCE f_u VS. INTERNAL FORCE f_i CONSIDERING σ_{ty} FOR 38.10 MM (1 ½ IN.) ROLLER AND POLYESTER GAUGE 142 AT THE TESTED VELOCITIES.	87

LIST OF TABLES

Table	Page
1. Experimental Data. Minimum load required to get wrinkling for 31.75mm (1 ¼ in.) roller, web: polyester gauge 48 and span: 381 mm.....	53
2. Experimental Data. Minimum load required to get wrinkling for 38.10 mm (1 ½ in.) roller, web: polyester gauge 48 and span: 381 mm.....	54
3. Web and roller surface roughness.....	55
4. Coefficient of friction web - roller.....	56
5. Theoretical wrinkling loads vs. mean values for experimental loads.....	85

NOMENCLATURE

a	half of web span
b	half of web width
CMD	cross machine direction
E_r	modulus of elasticity of the roller material
E_w	modulus of elasticity of the web material
f	distributed tension on the roller due to the web traction
fpm	feet per minute
f_μ	lateral surface force per unit length
f_i	lateral internal force per unit length
h_o	air film layer between web and roller
I_r	area moment of inertia for thin roller
M	bending moment
MD	machine direction
P	pressure onto the roller due to the web traction
PVC	polyvinyl chloride
q	parabolic web traction

R	outer radius of the roller
R_q	equivalent root mean square roughness
$R_{q,roller}$	roller surface roughness
$R_{q,web}$	web surface roughness
R_w	net force due to the web traction
$R_w \text{ exp.}$	experimental net force due to the web traction
$R_w \text{ theor.}$	theoretical net force due to the web traction
$S1 \ \& \ S2$	numerical coefficients of the parabolic web traction
T	web tension
t_w	web thickness
u_r	roller deflection in x direction
$u_r \text{ exp.}$	experimental roller deflection in x direction
$u_r \text{ theor.}$	theoretical roller deflection in x direction
V	shear force
x	distance along the machine direction
y	distance along the cross machine direction
$\alpha 1, \alpha 2 \ \& \ \alpha 3$	constants of the airy stress function
ε_x	web strain in the machine direction
$\phi(x, y)$	stress function

φ_w	wrapping angle
μ	coefficient of friction between web and roller
μ_{st}	static coefficient of friction between web and roller
v	web velocity
π	potential energy
θ	slope of the deflected roller
ϑ	dynamic viscosity of the air
σ_x	normal web stress in the machine direction
σ_{xy}	web shear stress
σ_y	normal web stress in the cross machine direction
ν	web's poisson ratio

CHAPTER 1

INTRODUCTION

A web is any material that is produced as a continuous, flexible, thin sheet able to withstand a high tensile stress, but unable to support a low compressive stress (1). Examples of webs include: material foil, polyester film, paper, and textiles.

Web manufacturing includes equipment functions requiring the web to be unwound, transported by rollers through different production steps, (such as printing, coating, laminating, etc.), and wound on a roller to be stored (2). During processing there are many opportunities for the web to obtain permanent defects that can affect the quality of the final product, thus producing high costs and material loss. Among those defects are wrinkles.

Wrinkles can be formed in the machine direction and/or in a direction not parallel to the machine direction. Wrinkles not aligned with the machine direction are called "shear wrinkles"(3). Good, Gehlbach and Kedl (3) have demonstrated that shear wrinkles are induced by lateral deformations, and hence shear on the web. Their research indicates the main reasons for deformations are mis-aligned rolls, controlled guide rolls, interaction roller-web, and web twist.

In the case of machine direction web wrinkling, Shelton (4) indicated that a lateral compressive strain/stress is responsible for wrinkle formation. This

compressive strain/stress may be produced by a roller deflection, a decrease in the tension across a driven roller, an increase in temperature and moisture, and the bending of a wound roll.

Shelton developed a theory of lateral compression for web wrinkles (4). According to Shelton's theory (4), in the case of web wrinkling due to roller deflection, there are two types of compressive stresses in the cross machine direction. The first type of the compressive stress causes wrinkles in a tensioned free web span. This stress is determined by the theory of elastic stability researched by Timoshenko and Gere (5) for a rectangular plate with uniform distributed load in the machine direction. The second stress is the lateral compressive stress that produces wrinkles in the web wrapping a roller. This stress is based on the theory of buckling of pressurized cylindrical shells (5). Shelton found that the critical compressive stress that buckles a web wrapping a roller is greater than the compressive stress that wrinkles a web span. For that reason, he concluded that one requirement of getting wrinkles in the web over a roller is to reach the buckling stress for a cylindrical shell without internal pressure.

Shelton's theory (4) goes on to indicate that the other condition required to maintain web wrinkles along the roller surface is the lateral surface force. This force is due to frictional contact with the web on the roller being greater than the compressive internal force due to buckling stress.

Duvall (6) performed several tests on a model based on Shelton's theory of buckling due to lateral forces caused by a deflecting roller. He found that the strains induced due to roller curvature were extremely high compared to the critical buckling strain. Duvall concluded that the maximum compressive strain due to bending on the top surface of the roller, matched with the experimental results.

Predicting web wrinkling is valuable in the web handling industry due to frustration, excessive costs, and the time involved with these defects. The purpose of this study is to develop a model to predict wrinkles in the machine direction in a web wrapping over a roller induced by roller deflection. Focusing on practical applications, the motivation is to develop a procedure based on simple equations. This application can be used in industry without requiring high-powered computers and sophisticated technology. To achieve that goal, and based on previous research, a web span is considered subjected to an assumed traction that causes a parabolic roller deflection. Expressions for web stress, web deformation in the machine direction, and roller deflection, among others, will be determined using energy methods and classical solid mechanics. Finally, theoretical wrinkling conditions will be established by enforcing compatibility between web-roller deformations and between the lateral compressive stress and buckling stress.

The experimental part of this study consists of building several flexible rollers for testing and a frame which was sufficient to support the required

instruments on the testing machine. Each roller will be deflected by a web tension obtaining web-wrinkling conditions over the roller. The correlation given among roller dimensions, roller properties, web dimensions, web properties, web span, web velocity and roller deflections will allow us to compare the experimental results to the theoretical computations and to determine a grade of accuracy of the proposed prediction model.

CHAPTER 2

THEORETICAL ANALYSIS

In web handling, roller deflections can be caused by web traction.

Considering the roller as a beam, for reasons of simple analysis and derivations, it has been verified that the parabolic shape is a reasonable approximation, even though the deflection curve is not exactly in the form of parabola (4). This geometry transfers a parabolic traction to the web when it conforms to the roller.

The objective of this chapter is to find a mathematical expression for the parabolic traction that produces simultaneously the same deformation at the roller and at the web under wrinkling conditions. To achieve that goal, we assume a polynomial expression for the web traction, this expression is composed of the numerical coefficients $S1$ and $S2$ which are functions of material properties and dimensional characteristics. Web span and roller deflection problems will be analyzed using the theory of elasticity. Based on Shelton's theory of lateral compression caused by roller deflection and other studies, the assumed parabolic traction will be verified for the inducement of wrinkle existence in the web wrapping over the roller.

2.1 Traction Boundary Valued Problem for a Web Span

Web spans can be analyzed using the criteria of two-dimensional elasticity in plane stress problems.

The geometry of a web is basically a thin plate or membrane with one dimension (thickness) much smaller than the others. The distributed load is applied over the thickness in the machine direction. In this case we consider no body forces in the plate problem.

The exact solution of two-dimensional problems in elasticity requires satisfying the following conditions: boundary conditions (kinematically admissible state), equilibrium conditions and compatibility equations(7).

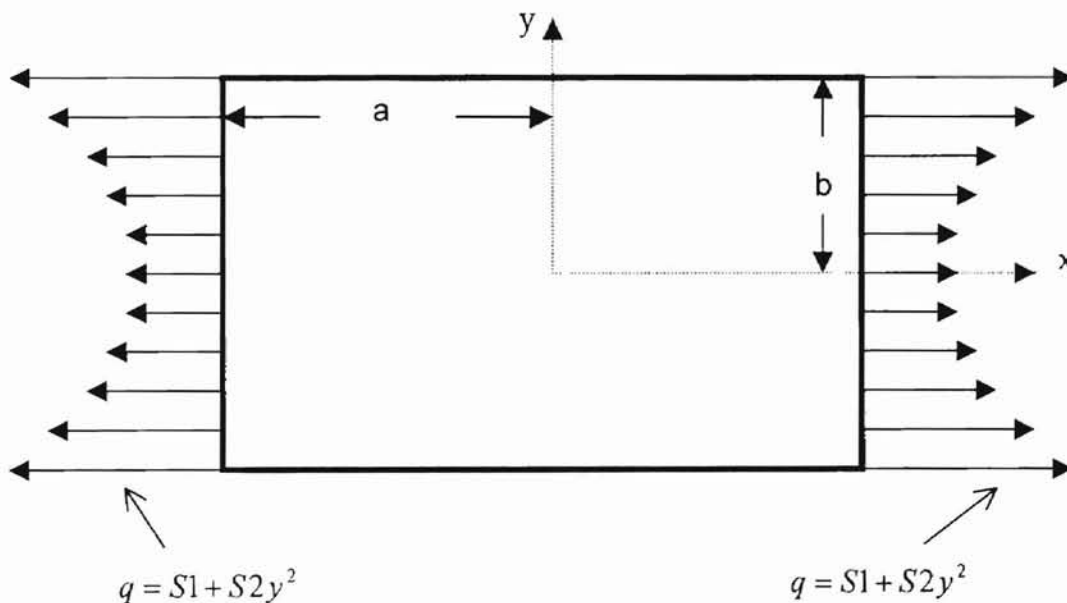


Figure 1. Web span modeled as a thin plate.

Figure 1 shows a web span modeled as a thin plate subjected to a parabolic distributed traction q . This web traction is assumed to have the following mathematical expression:

$$q = S1 + S2y^2 \quad [1]$$

where $S1$ and $S2$ are numerical coefficients.

Rivello (8) obtained an approximate solution for a plane stress plate problem with a pure parabolic traction in the form of a polynomial term (the parabolic traction) plus an infinite series. Rivello's stress function was modified in order to introduce our more general parabolic web traction as follows:

$$\phi = \frac{S1y^2}{2} + \frac{S2y^4}{12} + (x^2 - a^2)^2 (y^2 - b^2)^2 (\alpha1 + \alpha2x^2 + \alpha3y^2 + \dots) \quad [2]$$

where $\alpha1$, $\alpha2$ and $\alpha3$ are undefined constants.

The two first terms satisfy the essential (traction) boundary condition, and the third term assures no more stresses on the boundary. The series was truncated after the first three terms $\alpha1$, $\alpha2$ and $\alpha3$.

From classic solid mechanics (7), we know that a stress function $\phi(x, y)$ is related to stress as follows:

The normal stress in the machine direction (MD) is determined by:

$$\sigma_x = \frac{\partial^2 \phi}{\partial y^2} \quad [3]$$

The normal stress in the cross machine direction (CMD) is determined by:

$$\sigma_y = \frac{\partial^2 \phi}{\partial x^2} \quad [4]$$

and the shear stress can be found by:

$$\sigma_{xy} = -\frac{\partial^2 \phi}{\partial x \partial y} \quad [5]$$

Now, the problem is oriented to find the values for the unknown coefficients in the approximate solution $\phi(x, y)$ for the plane stress problem.

2.1.1 Principle of complementary strain energy. Rayleigh-Ritz method.

We shall now consider how the energy principles can be used to obtain the values of the coefficients α_1, α_2 & α_3 in the stress function $\phi(x, y)$ [2]. The procedure, known as the Rayleigh-Ritz method will be used with the principle of

complementary strain energy. The web will be considered as an isotropic homogeneous linearly elastic material.

The expression for the Complementary Energy “ π ” in the case of the plane stress problem without body forces is given by Rivello (8). Considering the web span as a region limited by $-a \leq x \leq a$ and $-b \leq y \leq b$, this expression becomes:

$$\pi = \frac{1}{E_w} \int_{-b}^b \int_{-a}^a [\sigma_x^2 + \sigma_y^2 - 2\sigma_x\sigma_y + 2(1+\nu)\sigma_{xy}^2] dx dy \quad [6]$$

where E_w is the modulus of elasticity of the web span and ν is the web's Poisson ratio.

By using equations [2], [3], [4] and [5], we derive the expressions for σ_x , σ_y & σ_{xy} which are then substituted into equation [6]. After integration, an expression is obtained for the complementary energy:

$$\pi = \frac{1}{2E_w} \left(\begin{aligned} & \frac{32768}{3675} \alpha^3 b^9 a^9 + \frac{32768}{75075} b^5 a^{13} \alpha^2 + \frac{131072}{11025} b^7 a^7 \alpha^2 + \frac{131072}{121275} b^7 \\ & a^{11} \alpha^2 + \frac{131072}{121275} \alpha^3 b^{11} a^7 + \frac{32768}{75075} \alpha^3 b^{13} a^5 + \frac{65536}{11025} b^9 a^7 \alpha^2 \alpha + \\ & \frac{1024}{1575} \alpha^3 b^7 S^2 a^5 + \frac{65536}{121275} \alpha^3 b^7 a^{11} \alpha^2 + \frac{4}{5} b^5 S^2 a + \frac{32768}{3675} \alpha^2 b^9 a^9 \\ & + 4bS^2 a + \frac{32768}{1575} b^5 a^9 \alpha^2 + \frac{32768}{1575} b^9 a^5 \alpha^2 + \frac{65536}{17325} b^{11} a^5 \alpha^3 \alpha + \\ & \frac{1024}{225} b^5 a^5 \alpha^2 \alpha + \frac{1024}{1575} + \frac{65536}{121275} b^{11} a^7 \alpha^2 \alpha^3 + \frac{65536}{11025} b^7 a^9 \alpha^3 \alpha + \\ & \frac{8}{3} b^3 S^2 a + \frac{65536}{17325} b^5 a^{11} \alpha^2 \alpha \end{aligned} \right) \quad [7]$$

The Rayleigh-Ritz method employs the theory of minimum total complementary potential (8). The total complementary strain energy is minimized with respect to the unknown coefficients in the stress function. Minimizing expression [7] with respect to α_1, α_2 & α_3 , we get a set of three algebraic equations as follows:

$$EQ_1 = \frac{\partial \pi}{\partial \alpha_1} = 0 \quad [8]$$

$$EQ_2 = \frac{\partial \pi}{\partial \alpha_2} = 0 \quad [9]$$

$$EQ_3 = \frac{\partial \pi}{\partial \alpha_3} = 0 \quad [10]$$

Solving the system of equation above yields the expressions for the coefficients α_1, α_2 & α_3 as follows:

$$\alpha_1 = -\frac{77 \left(1430a^8 + 9477a^6b^2 + 74219a^4b^4 + 9477a^2b^6 + 1430b^8 \right) S_2}{64 \left(\begin{array}{l} 25025a^{12} + 129740b^2a^{10} + 911998b^4a^8 + 726044b^6a^6 + \\ 911998b^8a^4 + 129740b^{10}a^2 + 25025b^{12} \end{array} \right)} \quad [11]$$

$$\alpha_2 = -\frac{1001 \left(715a^6 + 1235b^2a^4 + 170b^4a^2 + 22b^6 \right) S_2}{64 \left(\begin{array}{l} 25025a^{12} + 129740b^2a^{10} + 911998b^4a^8 + 726044b^6a^6 + \\ 911998b^8a^4 + 129740b^{10}a^2 + 25025b^{12} \end{array} \right)} \quad [12]$$

$$\alpha_3 = -\frac{1001 \left(22a^6 + 170b^2a^4 + 1235b^4a^2 + 715b^6 \right) S_2}{64 \left(\begin{array}{l} 25025a^{12} + 129740b^2a^{10} + 911998b^4a^8 + 726044b^6a^6 + \\ 911998b^8a^4 + 129740b^{10}a^2 + 25025b^{12} \end{array} \right)} \quad [13]$$

By substituting expressions [11], [12] and [13] into the equation [2] we will have determined an approximate solution for a web span subjected to a parabolic traction.

2.1.2 Expressions for normal stresses, strain and deformation in the machine direction for a web span.

Expressions for internal normal stresses in this web span problem can be found by substituting the above determined approximate solution $\phi(x, y)$ [2] into equations [3] and [4] as follows:

The internal stress in the machine direction (MD) is:

$$\sigma_x = S1 + S2y^2 + 8(x^2 - a^2)^2 y^2 (\alpha1 + \alpha2x^2 + \alpha3y^2) + 16(x^2 - a^2)^2 (y^2 - b^2) + \alpha3y^2 + 4(x^2 - a^2)^2 (y^2 - b^2) (\alpha1 + \alpha2x^2 + \alpha3y^2) + 2(x^2 - a^2)^2 (y^2 - b^2)^2 \alpha3 \quad [14]$$

The internal stress in the cross machine direction (CMD) is:

$$\sigma_y = 8x^2 (y^2 - b^2)^2 (\alpha1 + \alpha2x^2 + \alpha3y^2) + 16(x^2 - a^2) (y^2 - b^2)^2 \alpha2x^2 + 4(x^2 - a^2) (y^2 - b^2)^2 (\alpha1 + \alpha2x^2 + \alpha3y^2) + 2(x^2 - a^2)^2 (y^2 - b^2)^2 \alpha2 \quad [15]$$

To find the expression for the strain in the machine direction, we use the stress-strain relationship for a plane stress problem:

$$\varepsilon_x = \frac{1}{E_w} (\sigma_x - \nu\sigma_y) \quad [16]$$

Substituting equations [14] and [15] into [16] yields:

$$\varepsilon_x = \frac{1}{E_w} \left\{ \begin{array}{l} S1 + S2y^2 + 8(x^2 - a^2)^2 y^2 (\alpha1 + \alpha2x^2 + \alpha3y^2) \\ + 16(x^2 - a^2)^2 (y^2 - b^2) + \alpha3y^2 + 4(x^2 - a^2)^2 (y^2 - b^2) \\ (\alpha1 + \alpha2x^2 + \alpha3y^2) + 2(x^2 - a^2)^2 (y^2 - b^2)^2 \alpha3 - \\ \left(\begin{array}{l} 8x^2 (y^2 - b^2)^2 (\alpha1 + \alpha2x^2 \alpha3y^2) + 16(x^2 - a^2) \\ \nu \left((y^2 - b^2)^2 \alpha2x^2 + 4(x^2 - a^2) (y^2 - b^2)^2 (\alpha1 + \alpha2x^2 \alpha3y^2) \right) \\ + 2(x^2 - a^2)^2 (y^2 - b^2)^2 \alpha2 \end{array} \right) \end{array} \right\} \quad [17]$$

Finally, the strain-displacement relationship in the machine direction is determined by the following equation:

$$\varepsilon_x = \frac{\partial u_w}{\partial x} \quad [18]$$

From equation [18], we find that the web deformation is expressed by:

$$u_w(x, y) = \int \varepsilon_x dx + f(y) \quad [19]$$

where $f(y)$ is a function only of y . Solving equation [19], taking into account that $f(y)=0$ due to the symmetry of the web span about the y axis (at $x=0$, $u_w=0$), leads to the following expression for web deformation in the machine direction:

$$u_w = \frac{1}{E_w} \left\{ \begin{aligned} & S1x + S2y^2 + 8y^2 \left[\frac{1}{7} \alpha 2x^7 + \frac{1}{5} (-2a^2 \alpha 2 + \alpha 1 + \alpha 3y^2) + \right. \\ & \left. \frac{1}{3} (a^4 \alpha 2 - 2a^2 (\alpha 1 + \alpha 3y^2) x^3 + a^4) \right] + \\ & 16(y^2 - b^2) \alpha 3y^2 \left(\frac{1}{5} x^5 - \frac{2}{3} a^2 x^3 + a^4 x \right) + \\ & 4(y^2 - b^2) \left[\frac{1}{7} \alpha 2x^7 + \frac{1}{5} (-2a^2 \alpha 2 + \alpha 1 + \alpha 3y^2) + \right. \\ & \left. \frac{1}{3} (a^4 \alpha 2 - 2a^2 (\alpha 1 + \alpha 3y^2) x^3 + a^4) \right] + \\ & 2(y^2 - b^2)^2 \alpha 3 \left(\frac{1}{5} x^5 - \frac{2}{3} a^2 x^3 + a^4 x \right) - \\ & \left[8(y^2 - b^2)^2 \left(\frac{1}{5} \alpha 2x^5 + \frac{1}{3} (\alpha 1 + \alpha 3y^2) x^3 \right) + 16(y^2 - b^2)^2 \right. \\ & \left. \alpha 2 \left(\frac{1}{5} x^5 - \frac{2}{3} a^2 x^3 \right) + 4(y^2 - b^2)^2 \right] \\ & \left[\frac{1}{5} \alpha 2x^5 + \frac{1}{3} (-a^2 \alpha 2 + \alpha 1 + \alpha 3y^2) x^3 - a^2 (\alpha 1 + \alpha 3y^2) x \right] \\ & \left. + 2(y^2 - b^2)^2 \alpha 2 \left(\frac{1}{5} x^5 - \frac{2}{3} a^2 x^3 + a^4 x \right) \right] \end{aligned} \right\} \quad [20]$$

2.2 Beam theory to predict roller deflection due to a web tension

To find the expression for the roller deflection caused by a web tension, we consider the equilibrium of a flexible beam subjected to a distributed load. A roller can be satisfactorily modeled as a beam simply supported at its ends. When no load is applied, the neutral axis of the roller lies along the y axis. Due to

the lateral web behavior, it is convenient to fix the origin of coordinates at the roller center (Figure 2).

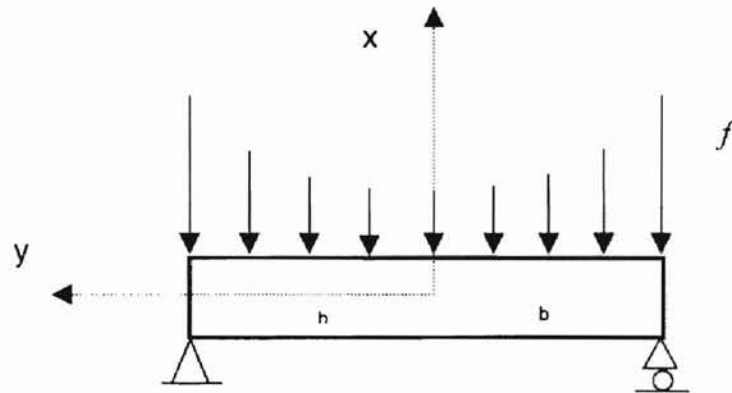


Figure 2. A roller subjected to a parabolic web tension f modeled as a simply supported beam.

Figure 3 shows a free body diagram for a roller subjected to a web tension T . The experimental apparatus used in this study set the wrapping angle ϕ_w at 180 degrees (figures 4 and 8 to 11).

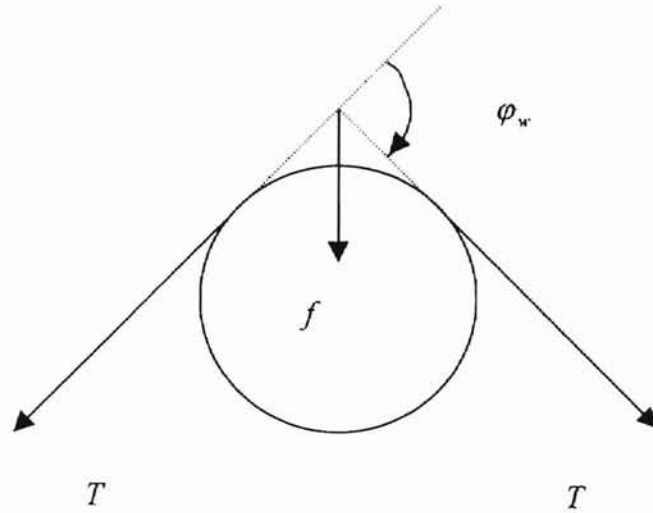


Figure 3. Forces acting over a roller due to web tension.

The assumed parabolic web traction q is varying with respect to the y axis. Hence, the expression for the distributed web tension f due to the web traction “ q ” becomes:

$$f = 2t_w (S_1 + S_2 y^2) \quad [21]$$

where t_w is the web thickness.

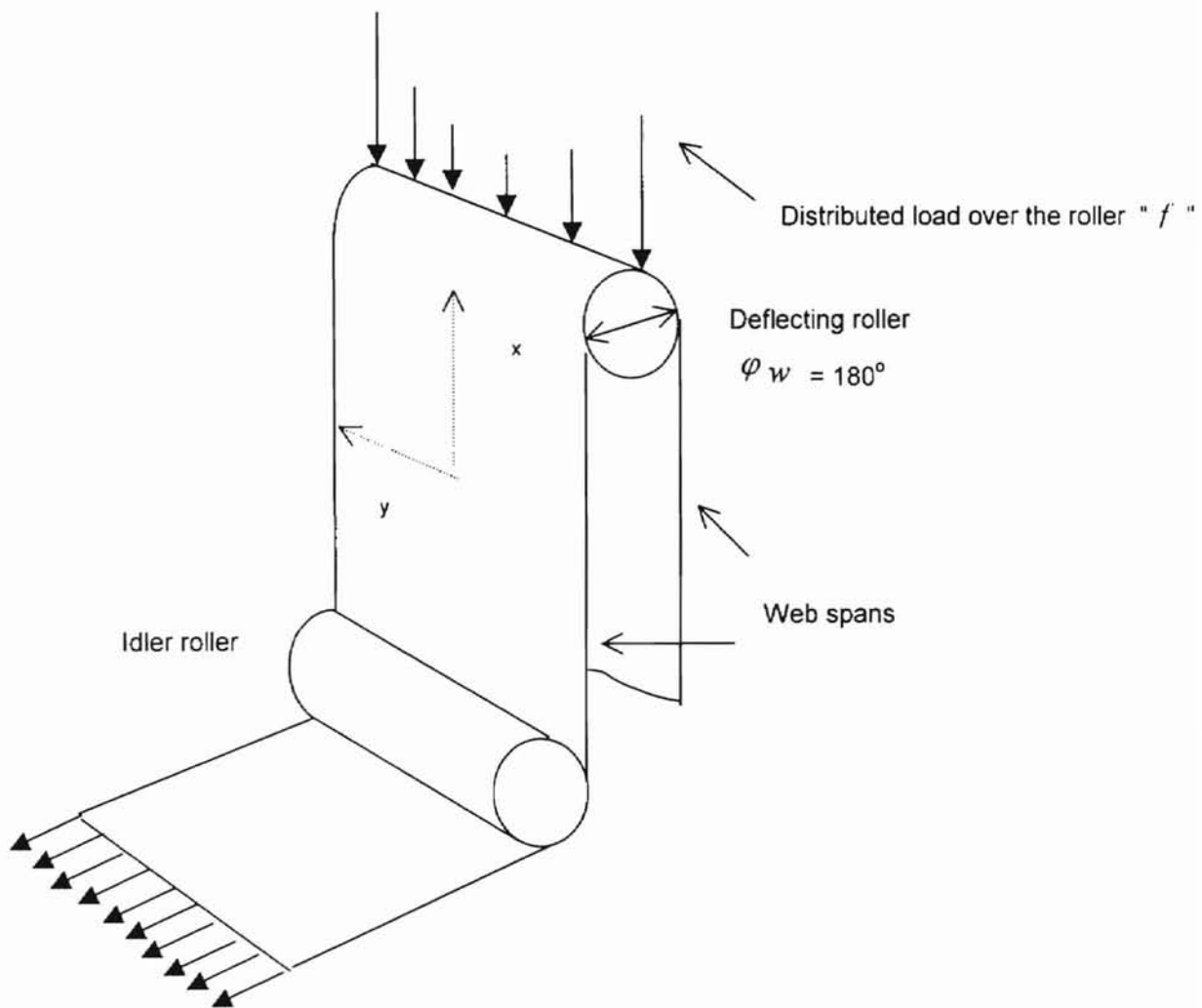


Figure 4. Test section.

In order to find the roller deflection, we will use the equilibrium equations for a distributed load on a beam, shear, bending moment and slope. For a roller of constant cross section, the beam equations are expressed as follows(7):

$$E_r I_r \frac{d^4 u_r}{dy^4} = f \quad [22]$$

$$E_r I_r \frac{d^3 u_r}{dy^3} = -V \quad [23]$$

$$E_r I_r \frac{d^2 u_r}{dy^2} = -M \quad [24]$$

$$\frac{du_r}{dy} = \theta \quad [25]$$

where u_r is the roller deflection, E_r is the modulus of elasticity of the roller material, I_r is the moment of inertia of the roller, V is the shear force, M is the bending moment and θ is the slope.

The net force F over the roller due the uniform distributed tension f is determined by:

$$F = - \int_{-b}^b 2t_w (S1 + S2y^2) dy = -4t_w b \left(S1 + \frac{S2b^2}{3} \right) \quad [26]$$

and the reactions at the simple supports becomes:

$$F_x = \frac{F}{2} = -2t_w b \left(S1 + \frac{S2b^2}{3} \right) \quad [27]$$

Substituting equation [21] into [22], integrating and then applying the boundary condition at $y = b$, $V =$ expression [27], yields:

$$\frac{d^3 u_r}{dy^3} = \frac{-2t_w}{E_r I_r} \left(S1y + \frac{S2y^3}{3} \right) \quad [28]$$

The expression for the bending moment M or curvature can be found integrating equation [28] and using the boundary condition at $y = b$, $M = 0$ as follows:

$$\frac{d^2 u_r}{dy^2} = \frac{1}{E_r I_r} \left[-2t_w \left(\frac{S1y^2}{2} + \frac{S2y^4}{12} \right) + \frac{t_w b^2}{6} (6S1 + S2b^2) \right] \quad [29]$$

The slope of the deflection curve is found by integrating equation [29] and enforcing the boundary condition of no slope at $y = 0$, as follows:

$$\frac{du_r}{dy} = -2t_w \left(\frac{S1y^3}{6} + \frac{S2y^5}{60} \right) + \frac{t_w b^2}{6} (6S1 + S2b^2)y \quad [30]$$

Finally, the equation for the roller deflection is determined by integrating equation [30] and enforcing the boundary condition $u_r = 0$ at $y = b$, as follows:

$$u_r = \frac{t_w}{E_r I_r} \left(-\frac{S1y^4}{12} - \frac{S2y^6}{180} + \frac{b^2 y^2 S1}{2} + \frac{b^4 y^2 S2}{12} - \frac{5b^4 S1}{12} - \frac{7b^6 S2}{90} \right) \quad [31]$$

2.3 Theory of lateral compression caused by roller deflection

Based on Timoshenko and Gere's theory of elastic stability (5), Shelton (4) reasoned that the lateral compression is caused by roller curvature; and that the lateral compressive stress responsible for wrinkles in a web, due to roller deflection, is the compressive stress that buckles the web wrapping a cylinder.

Timoshenko and Gere (5) studied the axial compression of a curved sheet panel. They determined, for the case of thin cylindrical shape, that the critical stress for symmetrical buckling with respect to the axis of the cylinder has the following expression:

$$\sigma_{cr} = \frac{E_w t_w}{R \sqrt{3(1-\nu^2)}} \quad [32]$$

where R is the nominal radius of the curved sheet and, also, of the outer surface of the roller.

The use of the above equation has been justified by Shelton (4) in the case of a web wrapping a roller, or the outer wraps of a wound roll.

Shelton, also, considered the effect of friction between a web and roller (4). For a web wrinkling over a roller, a reaction force is required to sustain the wrinkled web upon the roller surface (9). This force is denominated as the lateral surface force f_μ and must be greater than the internal force f_i due to the lateral

compressive buckling stress acting on the web, for a wrinkle to be sustained in the web as it crosses a roller.

When the pressure P between the web and roller is constant, the maximum lateral surface force f_μ is equal to the pressure P multiplied by the contact area and by the coefficient of friction μ between web and roller(4).

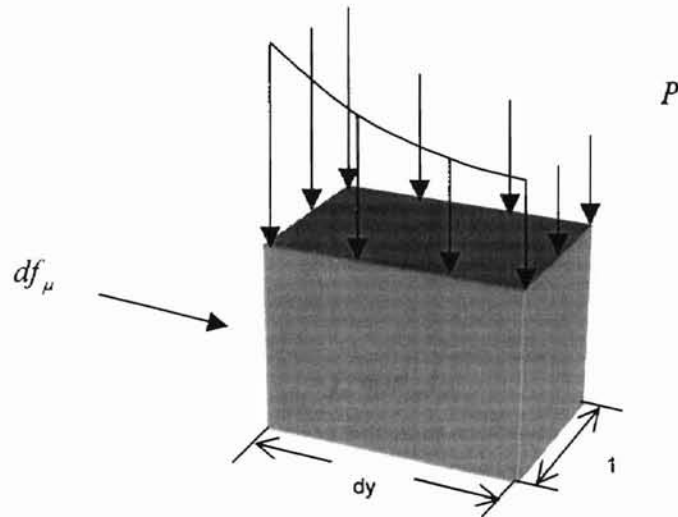


Figure 5. Schematic of an elemental web piece at the contact area web-roller.

Figure 5 shows an elemental piece of web of the contact area between the web and roller; using the given definition for the lateral surface force, we get:

$$df_\mu = \mu P dy \quad [33]$$

where P is given by the equilibrium equations for a thin wall pressure vessel, as follows:

$$P = \frac{\sigma_x t_w}{R} = \frac{(S1 + S2y^2) t_w}{R} \quad [34]$$

Therefore, substituting equation [34] into [33] and considering symmetry about the x axis, we can get the expression for the lateral surface force f_μ per unit wrap length as follows:

$$f_\mu = \frac{\mu t_w}{R} \int_0^b (S1 + S2y^2) dy \quad [35]$$

The expression for the maximum lateral compressive internal force f_i due to buckling is given by:

$$f_i = \sigma_{cr} t_w \quad [36]$$

where σ_{cr} is the critical buckling stress obtained by equation [32].

2.3.1 Effect of the air film layer h_0 on the coefficient of friction between web and roller.

Knox and Sweeney (10) demonstrated the existences of an air film layer h_0 between web and roller due to hydrodynamic lubrication. They developed the following expression:

$$h_0 = 0.65R \left(\frac{12\theta v}{T_w} \right)^{\frac{2}{3}} \quad [37]$$

where \mathcal{G} is the dynamic viscosity of the air ($3.077 \cdot 10^{-7}$ N-min/m² @ 27 °C), v is the web velocity (m/min) and T_w is the web tension.

In the case of parabolic web traction “ q ”, the equation [37] becomes:

$$h_0 = 0.65R \left[\frac{12.9v}{(S1 + S2y^2)T_w} \right]^{\frac{2}{3}} \quad [38]$$

Good, Kedl and Shelton (9) analyzed the effect of the air film layer h_0 on the behavior of the coefficient of friction μ . They developed an algorithm which relates h_0 , the equivalent root mean square roughness R_q

($Rq = \sqrt{R_{q,roller}^2 + R_{q,web}^2}$) and the static coefficient of friction μ_{st} to μ . The algorithm is expressed as follows:

$$\begin{aligned} R_q &\geq h_0 & \mu &= \mu_{st} \\ 3R_q &\geq h_0 \geq R_q & \mu &= \mu_{st} \left(1.5 - \frac{h_0}{2R_q} \right) \\ h_0 &\geq 3R_q & \mu &= 0 \end{aligned} \quad [39]$$

Therefore, f_μ per equation [35] may be affected depending on the value of the air film h_0 along the web width.

Duvall (6) found that his experimental results did not obey the theory developed by Shelton. The experimental results matched better with the assumption that the web assumes the shape of the deflected roller and hence induced bending stresses in the shell of web upon the roller. Therefore, an

additional condition of compatibility between web and roller deformations should be considered for wrinkle formation.

2.4 Minimum parabolic traction that causes web wrinkling due to roller curvature.

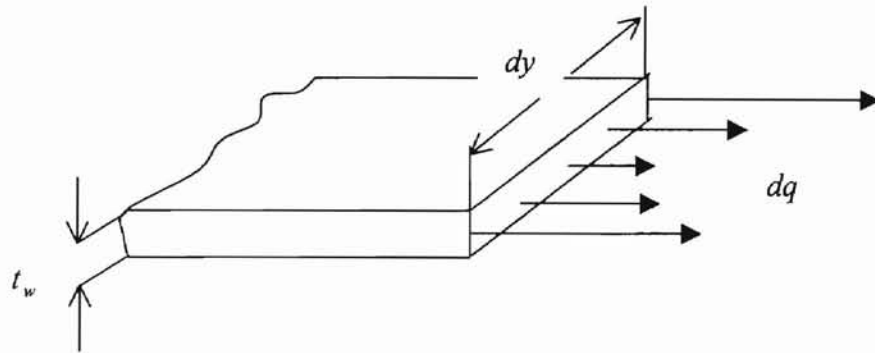


Figure 6. Schematic of an elemental parabolic web traction d_q applied on an elemental web width.

Recalling the assumed expression for the parabolic web traction (equation [1]) and based on figure 6, the expression for the net force applied, R_w , due to the parabolic distributed traction can be determined as follows:

$$R_w = \int_{-b}^b t_w (S_1 + S_2 y^2) dy = 2 t_w b \left(S_1 + \frac{S_2 b^2}{3} \right) \quad [40]$$

Equation [40] represents the relationship between the necessary load to transport the web R_w and the coefficients S_1 and S_2 which define the parabolic distribution of the traction along the web width.

2.4.1 Methodology to predict the minimum parabolic web traction that causes wrinkling due to roller curvature.

The objective of this part of the research is to describe the proposed model to predict the critical parabolic web traction for wrinkling due to roller deflection. The iterative method was used during the theoretical computation in this work. To perform it, a spreadsheet in the software EXCEL was utilized and the iterative process was accomplished using the command SOLVER.

Step 1: Imaginary points along the contact line web-roller.

We will consider divided the contact line between the web span and the deflected roller into equidistant n -points. This will assure full contact between the roller length and the web width.

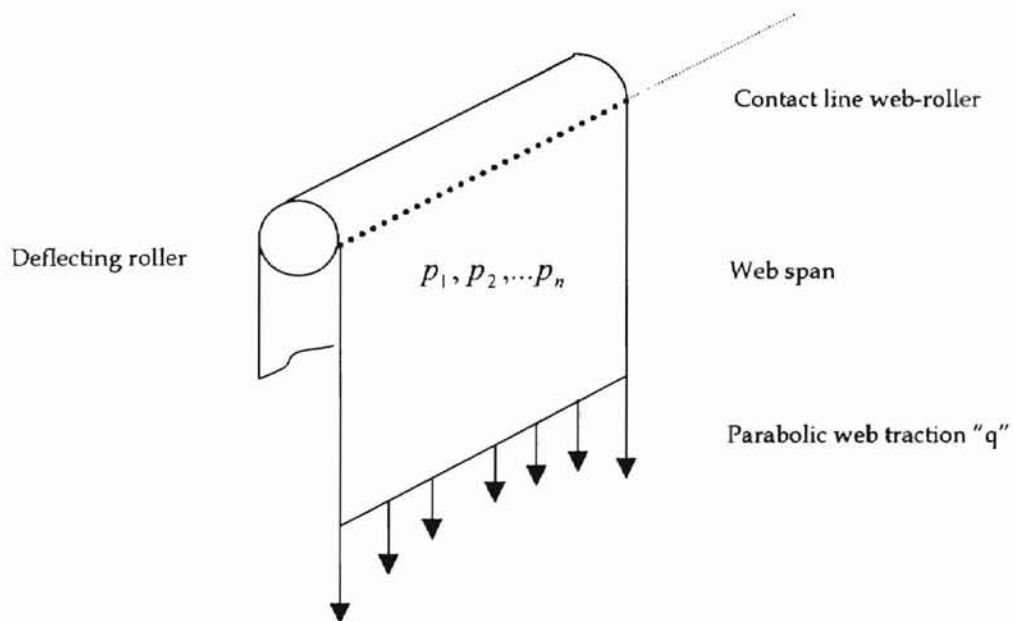


Figure 7. Imaginary points along the contact line web-roller.

Step 2: Estimation of R_w and $S2$

Now, an iterative process will be performed. It begins with the assumption of a load R_w and a coefficient $S2$. The coefficient $S1$ can be determined using equation [40].

Step 3: Maximum compressive stress in CMD σ_y :

With $S1$ & $S2$ from step 2 and using equation [15], the internal web stress in the cross machine direction for each point p_1, p_2, \dots, p_n can be computed. It is expected that the maximum σ_y being located at the center point on the contact line web-roller.

Step 4: Critical buckling stress σ_{cr} .

The critical compressive stress for buckling will be determined by equation [32].

Step 5: Web deformation at the contact line web-roller u_w .

With $S1$ & $S2$ from step 2 and using equation [20], the web deformation for each point p_1, p_2, \dots, p_n can be found.

Step 6: Roller deflection u_r .

Substituting $S1$ & $S2$ into equation [31] will allow us to compute the roller deflection for each point p_1, p_2, \dots, p_n along the contact line web-roller.

Step 7: Compatibility between roller deflection u_r and web deformation

$$u_w.$$

Next, we determine the error or difference between the web deformation and the roller deflection for each point p_1, p_2, \dots, p_n . The summation of errors will be referred to as compatibility error or sum-error.

Step 8: Lateral surface force per unit length $f\mu$.

Substituting $S1$ & $S2$ into equation [38], the air film thickness h_0 for each point p_1, p_2, \dots, p_n will be found. According to the algorithm [39], the lateral surface force per unit length can be determined using equation [35].

Step 9: Lateral compressive force per unit length f_l .

The lateral compressive force per unit length can be calculated by equation [36].

Step 10: Stress wrinkling condition.

Is the maximum σ_y obtained in step 3 equal to σ_{cr} given by step 4?

If YES go to step 11.

If NO go to step 2.

Step 11: Compatibility wrinkling condition.

Is sum-error or compatibility error in step 7 negligible (less than 1-2%)?

If YES go to step 12.

If NO go to step 2 and assume a new value for $S2$.

Step 12: Frictional wrinkling condition.

Is $f\mu$ obtained in step 8 greater than f_l given in step 9?

If YES, R_w is the minimum net wrinkling load to be applied in web handling equipment. $S1$ & $S2$ are the coefficients that when placed into the equation [1], describe the minimum parabolic web traction responsible to wrinkle the web that wraps a roller due to roller deflection.

If NO go to step 2 and increment R_w

CHAPTER 3

EXPERIMENTAL SETUP AND PROCEDURE

The objective of this part of the study is to describe the steps taken during the experimental process of this research. It covers a brief description of the testing machine, material selection, roller design based on initial estimations, and a description of the experimental procedure.

3.1 Testing machine

Web wrinkling experiments were performed in the Web Handling Research Center at OSU. The testing machine is shown below in Figures 8 to 10.

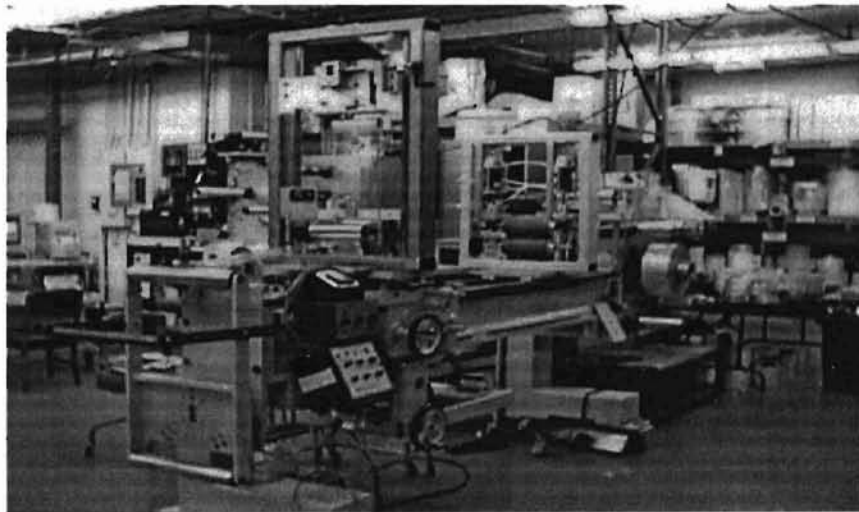


Figure 8. Testing Machine in the WHRC at OSU.

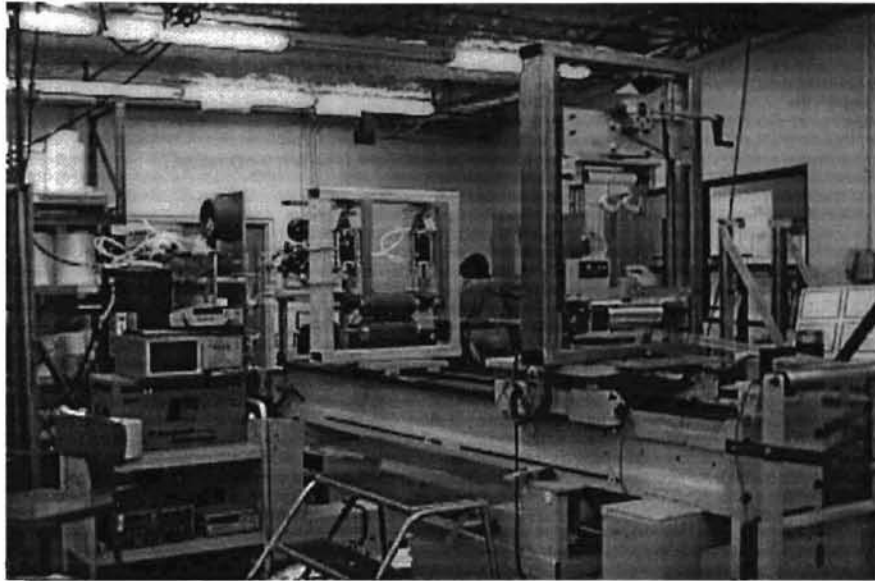


Figure 9. Testing Machine in the WHRC at OSU.

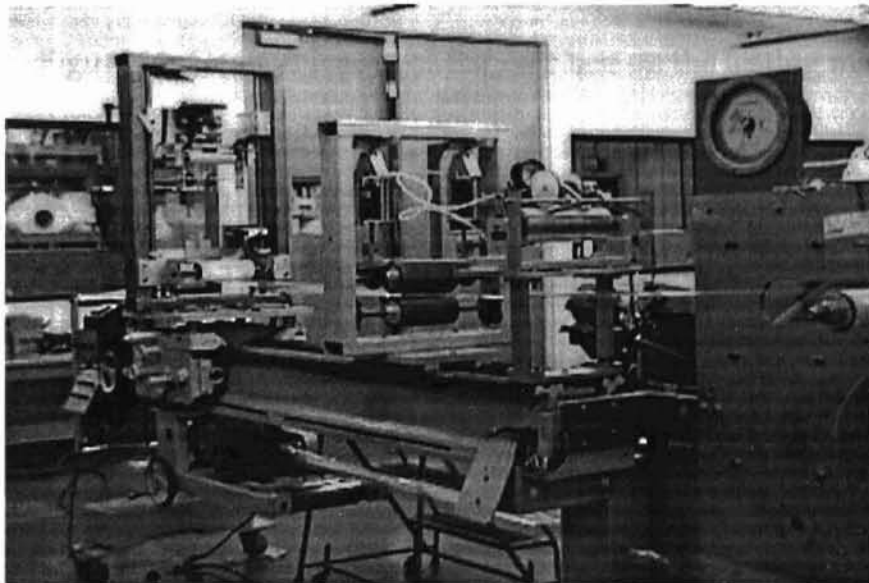


Figure 10. Testing Machine in the WHRC at OSU.

The general layout of the web on the testing machine is shown in Figure

11.

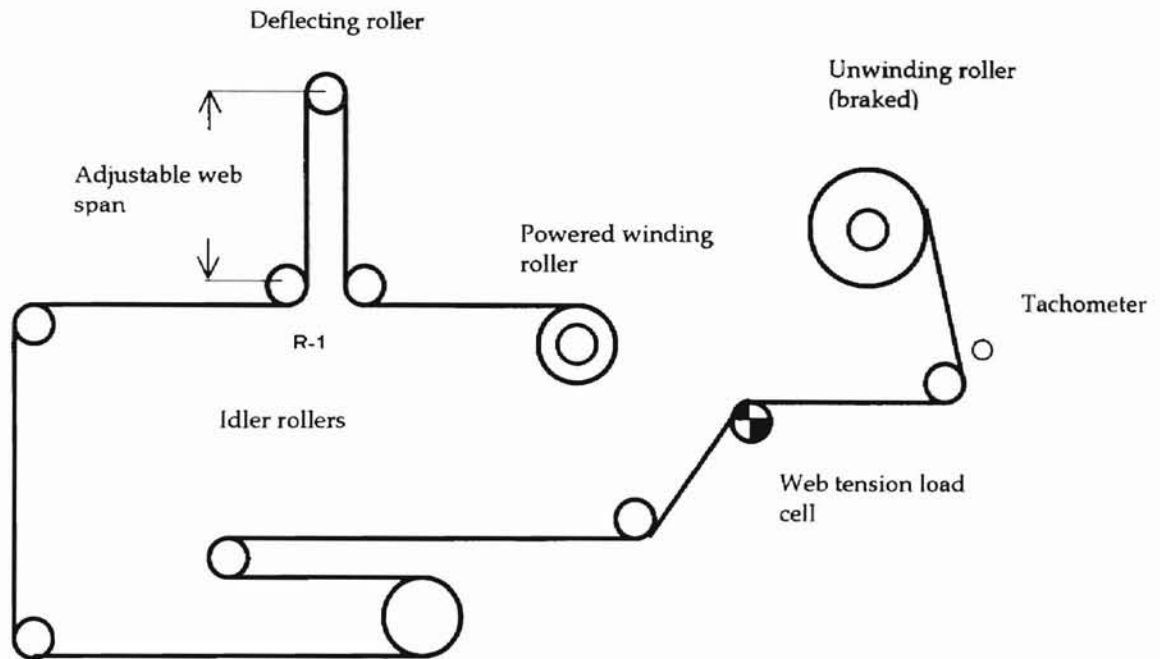


Figure 11. General layout of the web line on the testing machine.

The experimental testing machine is able to produce a maximum tensile load of 89 N (20 lbf). This load is created by an adjustable magnetic brake system at the unwinding roller. The desired value of the load is the result of the tension difference between the powered winding roller and the required brake during the unwinding operation. The applied tensile load over the web can be monitored in a digital tension readout indicator with a resolution no less than 1/10 lbf. This indicator receives the corresponding signal from a tension transducer located at the idler roller R-1 (Figure 11).

The web velocity is set in a digital panel that controls the speed of the powered winding roller. During the experiments, the minimum testing velocity was of the order of 13 m/min (40 fpm) and the maximum of the order of 40 m/min (130 fpm). The web span between the deflecting roller and the idler rollers can be adjusted manually. This testing machine has a minimum web span of 254 mm (10 in.) and a maximum value of 610 mm (24 in.); however, those web span limits may vary depending on the roller sizes. The web spans chosen in this study were 381 mm (15 in.) and 508 mm (20 in.). As mentioned previously, all experiments were done using an angle of wrap of 180 degrees.

3.2 Web properties and dimensions.

Web wrinkling tests were performed on films with the following characteristics:

Material: Polyester.

Modulus of elasticity (E_w): 4140 MPa (600468 psi)

Poisson's ratio: 0.3

Web width: 152.4 mm (6 in.)

Web thickness: a - Gauge 48 (12 Microns or $4.72 \cdot 10^{-4}$ in.)

b- Gauge 92 (23 Microns or $9 \cdot 10^{-4}$ in.)

c- Gauge 142 (36 Microns or $1.4 \cdot 10^{-3}$ in.)

3.3 Roller properties and dimensions.

Roller design started with the material selection. Several factors had an influence in making this decision. Among them were: a desired considerable material flexibility, testing machine limitations (e.g. max. tensile load = 89 N (20 lbf.)), costs, availability, and weight. PVC pipe having a Young's modulus of approximately 1800 MPa (261000 psi) was selected.

In order to find the proper outer diameter and wall thickness of the roller, initial estimations were made taking into consideration the following conditions: maximum testing load = 89 N (20 lbf), roller length equals to the web width, a desired low roller stiffness, web spans of 381 mm (15 in.) and 508 mm (20 in.), and the material's ability to cause wrinkles.

The result was the following three rollers: a) Nominal diameter of 31.75 mm (1 ¼ in.), schedule 20, b) Nominal diameter of 38.10 mm (1 ½ in.) schedule 20, and c) Nominal diameter of 50.80 mm (2 in.), schedule 20.

The study of the roller deflections was necessary in this research. The experimental roller deflections were measured with two micrometers with a resolution of 1/100 mm or 5/10000 inch. One micrometer was located so that it could measure the deflection at roller center. The other micrometer was able to detect the deflection at the roller edge, note Figure 12.

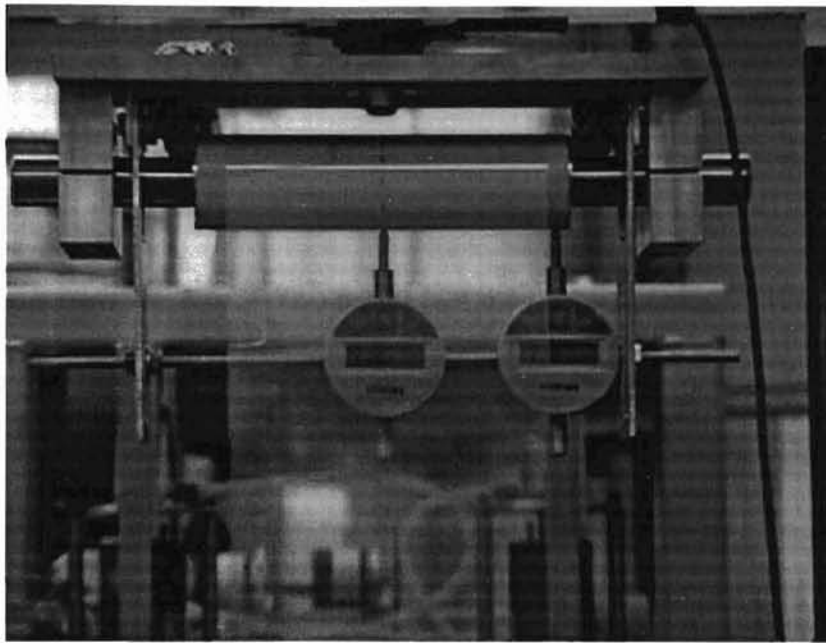


Figure 12. 31.75 mm (1 ½ in.) roller assembled with the two micrometers on the testing machine. Web is Polyester gauge 92.

3.4 Experimental Procedure.

Having fully defined web and roller characteristics, each roller was tested on the testing machine using different thickness polyester films. The experimental procedure follows:

For a given roller size, polyester film and a fixed web span, each test began by setting the web tensile load and web velocity. Then, progressively, the web tension was increased in intervals of approximately 2 lbf until a wrinkle formed in the web wrapping the deflecting roller. The wrinkling load was

recorded from readings in the digital tension readout and the roller deflections from the micrometers.

After that, the applied tension was reduced to a minimum value. The velocity was set to a new value and the web load was increased again until the new minimum load to form wrinkles was found.

The same procedure was repeated for each roller size, polyester caliper and web span. The data obtained were processed in order to compare with the theoretical computations obtained under the same conditions.

3.5 Web and roller surface roughness

The surface roughness of the tested polyester films is an important property used to determine the lateral surface force $f\mu$ by algorithm [39]. For that reason each type of polyester film (gauge 48, 92 and 142) was tested in the Web Handling Research Center using a " Surfctest Analyzer and Surfctest 402 " a surface profilometer manufactured by Mitutoyo Corporation. Pieces of web were located on a very smooth surface (glass) and several surface roughness readings were obtained.

Similar to the surface roughness tests done on the polyester films, the surface roughness of the rollers were obtained using the Surfatest Analyzer. Data

along lines parallel to the cylindrical axis at the external surface of the rollers were recorded.

3.6 Coefficient of friction between web and roller.

Several tests were conducted in order to measure the experimental coefficient of friction between the web and roller surfaces. These tests consisted of registering the maximum load just when the slippage impediment between the web and roller was broken. Using the brand-brake equation, we could find the value of the respective coefficient of friction.

$$\mu_{st} = \frac{1}{\varphi_w} \ln \frac{P_1}{P_2} \quad [41]$$

where P_1 is the maximum force to break the slippage impediment, P_2 is the weight of a dummy body, φ_w is the angle of wrap of the web over the roller and μ_{st} is the static coefficient of friction.

CHAPTER 4

EXPERIMENTAL RESULTS

4.1 Experimental Wrinkling Conditions

After performing several experiments, web wrinkles were formed on each of the tested rollers and the polyester films at different spans and velocities. The only exception was the 50.80 mm (2 in.) roller. This roller only allowed wrinkle existence for polyester gauge 48, web span of 381 mm (15 in.) and speed of 13 m/min (42 fpm).

It was noted that prior to wrinkle formation at the web over the roller, many troughs appeared at the web span (Figure 13). It confirmed what Shelton (4) established. The compressive stress that buckles the web wrapping a roller is greater than the compressive stress that wrinkles a web span.

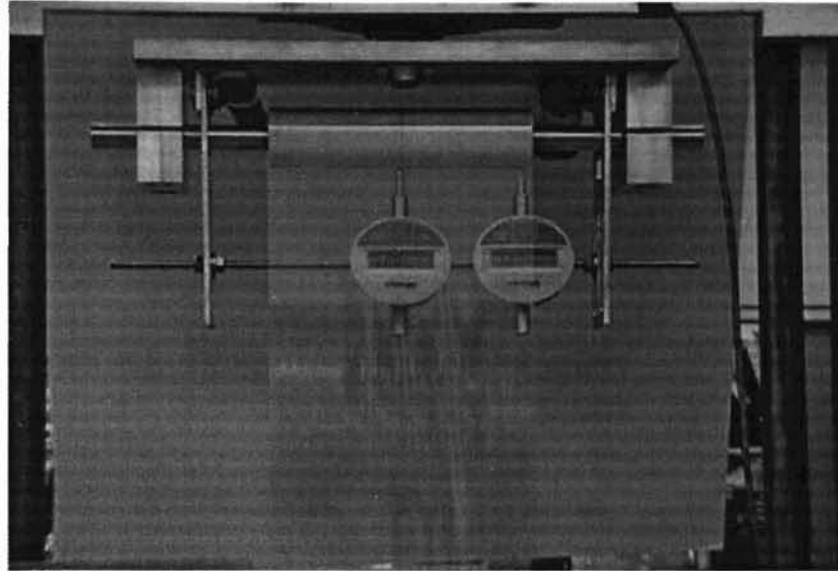


Figure 13. Troughs at the web span before wrinkling formation in the web wrapping the roller. Note that even though the span has troughs, the web wrapping the roller is uncorrugated. Roller: 31.75 mm (1 ¼ in.), web: Polyester gauge 48, span: 508 mm (20 in.) and velocity: 14 m/min (47 fpm).

During the tests, wrinkles over the deflecting roller initially appeared approximately at the central region of the roller. Then, they moved from the roller center to the left roller edge or right roller edge. At the edges, the wrinkles disappeared to repeat the cycle with a new wrinkle. Only wrinkles in the machine direction were formed during these experiments. Figures 14 to 18 show several examples of web wrinkles that were formed during the experimental part of this research.

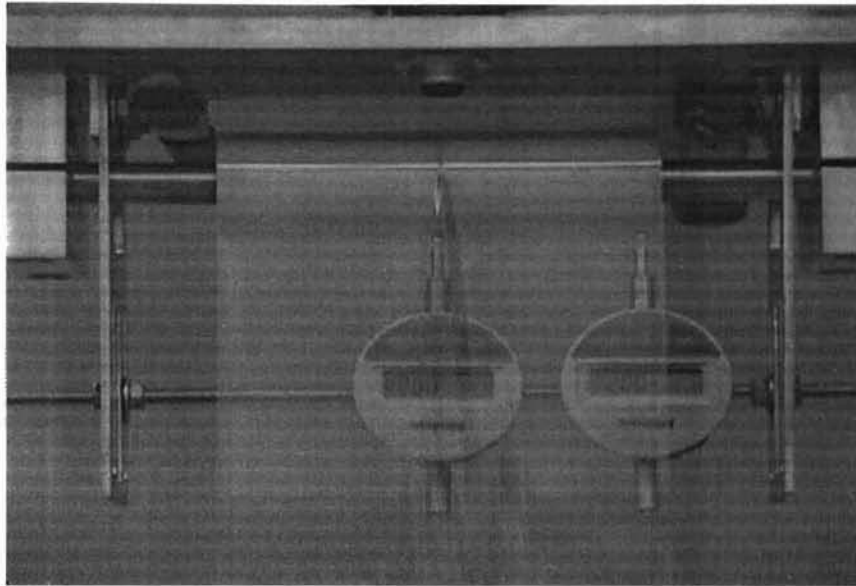


Figure 14. Initial wrinkling formation. Wrinkle initially appeared at the roller center. Roller: 31.75 mm (1 ¼ in.), Polyester gauge 48, span: 508 mm (20 in.) and velocity: 14 m/min (47 fpm).

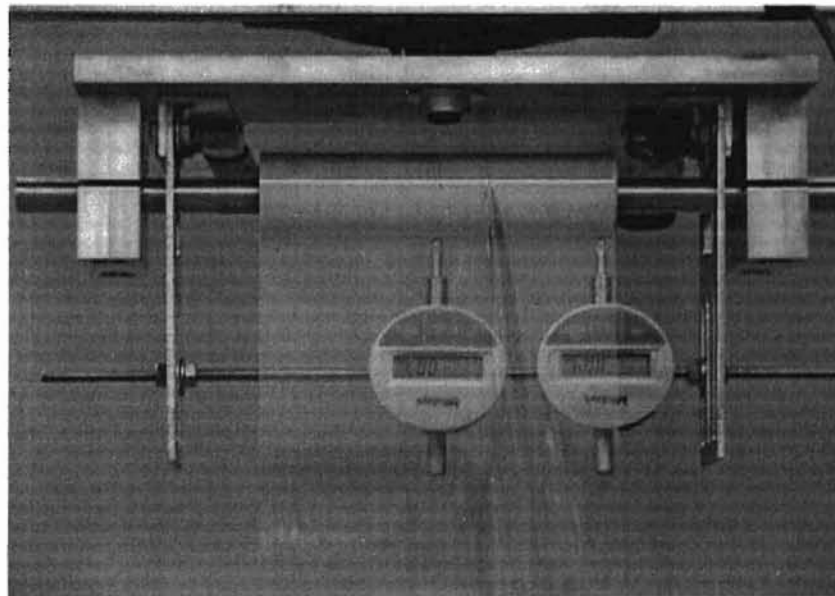


Figure 15. Web wrinkling over the roller. Note how the wrinkle initially at the roller center is moving to the roller edge. Roller: 31.75 mm (1 ¼ in.), Polyester gauge 48, span: 508 mm (20 in.) and velocity: 14 m/min (47 fpm).

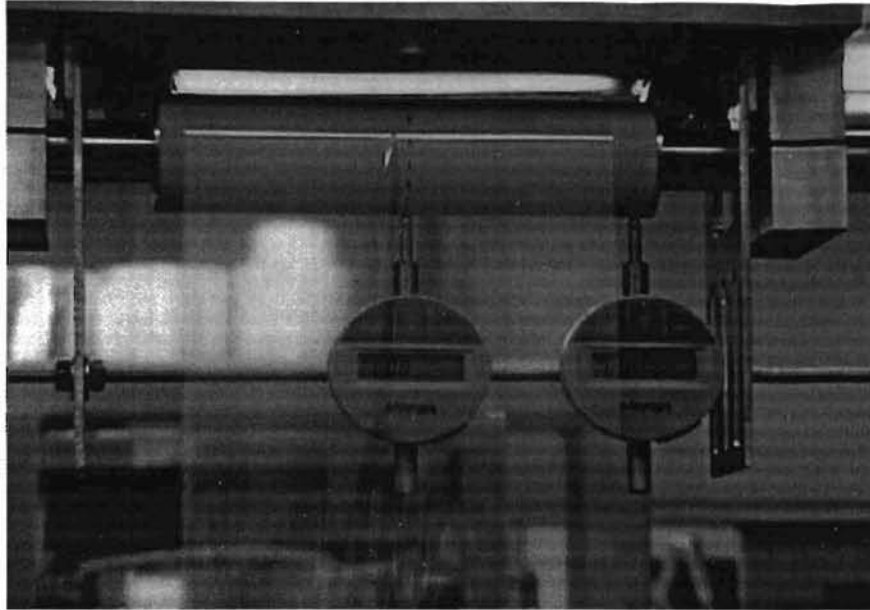


Figure 16. Initial wrinkling formation on the 38.10 mm (1 ½ in.) roller, Polyester gauge 92, span: 508 mm (20 in.) and velocity: 29 m/min (95 fpm). Wrinkles were initially formed at the center of the web.

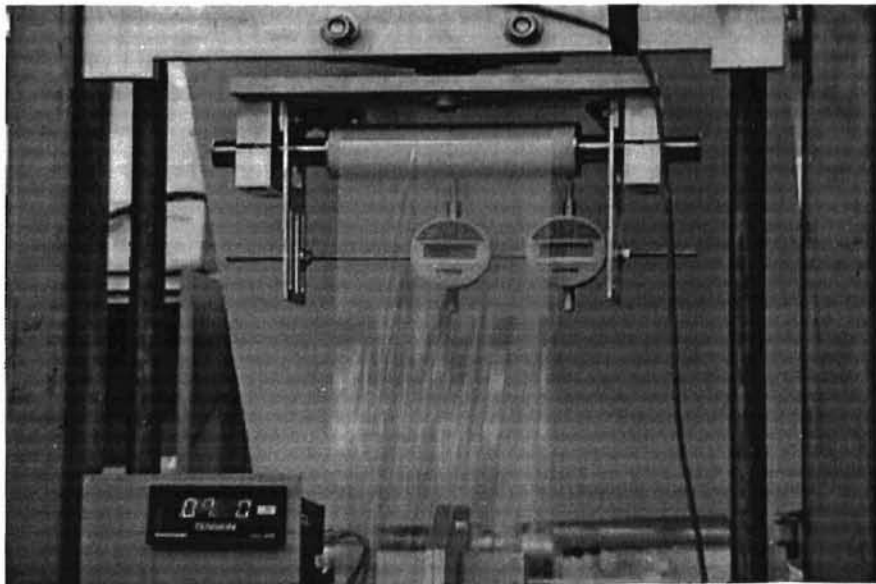


Figure 17. Web wrinkling over the 38.10 mm (1 ½ in.) roller, Polyester gauge 48, span: 508 mm (20 in.) and velocity: 29 m/min (95 fpm).

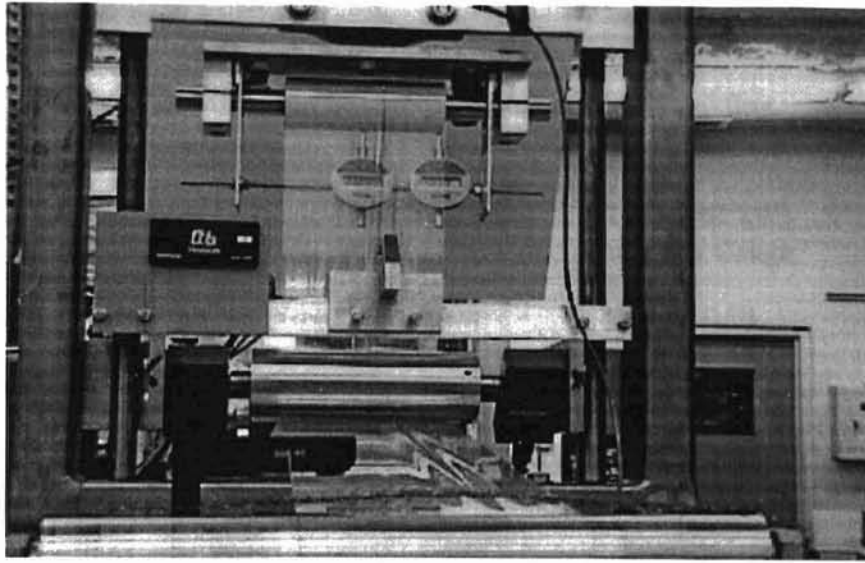


Figure 18. Web wrinkling over the 50.80 mm (2 in.) roller, Polyester gauge 48, span: 381 mm (15 in.) and velocity 13 m/min (42 fpm).

The experimental data obtained from the performed tests were recorded in tables in order to be analyzed and compared with the theoretical calculations.

The recorded data were the minimum experimental tensile loads required to wrinkle the web films over the roller and the deflections at the roller edge and at the center.

Each of the tables shows the experimental data for a particular web span and web caliper tested to a set of three different web speeds. The relative center deflections (difference between roller deflections at the center and at the edge) are also indicated. As an example, Tables 1 and 2 are displayed in the following pages. They indicate the experimental data for 31.75 mm (1 ¼ in.) and 38.10 mm (1 ½ in.) rollers at web span of 381 mm (15 in.).

Table 1
Minimum Load required to get Web Wrinkling
Experimental Data

Roller : 31.75 mm(1 1/4")
 Web: Polyester Gauge 48
 Web Span: 381 mm (15")

a) Web velocity= 14.32 m/min

Test	Experimental load (N)	Center deflection (mm)	Edge deflection (mm)	Relative center deflection (mm)
1	15.12	0.03	0.01	0.02
2	13.80	0.03	0.01	0.02
3	12.45	0.03	0.01	0.02
4	16.45	0.03	0.01	0.02
5	16.01	0.03	0.01	0.02
6	19.26	0.04	0.01	0.03
7	17.35	0.04	0.01	0.03

b) Web velocity= 29 m/min

Test	Experimental load (N)	Center deflection (mm)	Edge deflection (mm)	Relative center deflection (mm)
1	21.00	0.04	0.01	0.03
2	22.24	0.04	0.01	0.03
3	22.00	0.04	0.01	0.03
4	17.40	0.04	0.01	0.03
5	22.70	0.04	0.01	0.03
6	18.00	0.04	0.01	0.03
7	18.70	0.04	0.01	0.03

c) Web velocity= 42.4 m/min

Test	Experimental load (N)	Center deflection (mm)	Edge deflection (mm)	Relative center deflection (mm)
1	23.13	0.04	0.01	0.03
2	24.02	0.04	0.01	0.03
3	21.00	0.04	0.01	0.03
4	22.70	0.04	0.01	0.03
5	22.24	0.04	0.01	0.03
6	21.35	0.04	0.01	0.03
7	23.60	0.04	0.01	0.03

Table 2
Minimum Load required to get Web Wrinkling
Experimental Data

Roller : 38.10 mm
 (1 1/2")
 Web: Polyester Gauge 48
 Web Span: 381 mm (15")

a) Web velocity= 13 m/min

Test	Experimental load (N)	Center deflection (mm)	Edge deflection (mm)	Relative center deflection (mm)
1	18.23	0.03	0.02	0.01
2	19.60	0.04	0.02	0.02
3	21.00	0.04	0.02	0.02
4	24.02	0.05	0.02	0.03
5	20.50	0.04	0.02	0.02
6	16.46	0.03	0.02	0.01

b) Web velocity= 27 m/min

Test	Experimental load (N)	Center deflection (mm)	Edge deflection (mm)	Relative center deflection (mm)
1	22.70	0.04	0.02	0.02
2	25.35	0.04	0.02	0.02
3	25.80	0.05	0.02	0.03
4	25.35	0.04	0.02	0.02
5	23.57	0.04	0.02	0.02
6	26.24	0.05	0.02	0.03

c) Web velocity= 41 m/min

Test	Experimental load (N)	Center deflection (mm)	Edge deflection (mm)	Relative center deflection (mm)
1	29.36	0.05	0.02	0.03
2	26.24	0.04	0.02	0.02
3	25.35	0.04	0.02	0.02
4	27.57	0.04	0.02	0.02
5	28.47	0.05	0.02	0.03
6	22.70	0.05	0.02	0.03

4.2 Experimental Web and Roller Roughness

Table 3 registers the experimental data obtained for the surface roughness of the different web calipers and tested rollers:

Table 3			
Web surface roughness " $R_{q, web}$ "			
(10 ⁻⁴ mm)			
Test	gauge 48	gauge 92	gauge 142
1	6.6	6.6	3.3
2	3.0	2.5	3.6
3	2.3	9.4	5.3
4	6.1	10.2	7.6
5	4.8	1.8	4.1
6	3.0	2.0	
7	3.3	5.8	
Average=	4.2	5.5	4.8
Roller surface roughness " $R_{q, roller}$ "			
(10 ⁻⁴ mm)			
Test	31.75mm diam.	38.10 mm diam.	50.80 mm diam.
1	15.2	10.9	8.9
2	15.0	19.8	14.5
3	17.5	12.2	18.3
Average=	15.9	14.3	13.9

4.3 Coefficient of Friction between Web and Roller

The following experimental table was obtained from the test performed on each roller and web caliper and using the brand-brake equation:

Test	Static Coeff.
1 1/4 "	0.24
1 1/2 "	0.27
2 "	0.30

CHAPTER 5

ANALYSIS OF EXPERIMENTAL DATA

5.1 Initial theoretical computations.

Initial theoretical computations were done based on the method described in 2.4.1 of Chapter 2. The goal of these calculations was to find simultaneous fulfillment of the theoretical wrinkling conditions (stress, compatibility and frictional).

The mathematical expressions to perform the initial computations for each roller diameter, web caliper, span and web speed are indicated in Chapter 2. The iterative process explained in the proposed methodology was accomplished by using a spreadsheet in the software EXCEL.

As an example of the initial computations, results and graphs for the case of 31.75 mm (1 ¼ in.) roller, polyester gauge 48, span of 381 mm (15 in.) and velocity of 14.32 m/min (47 fpm) are given below:

Results of Theoretical Computations

Roller: PVC Diam.: 31.75 mm, Web: Polyester, gauge 48, Span: 381 mm

Web veloc.= 13 m/min

Min. Load (Rw theor.)= 9.11 Lbf or 40.51 Newtons

Traction Coeff. S1= 20.69 N/mm² and S2= 0.0008 N/mm⁴

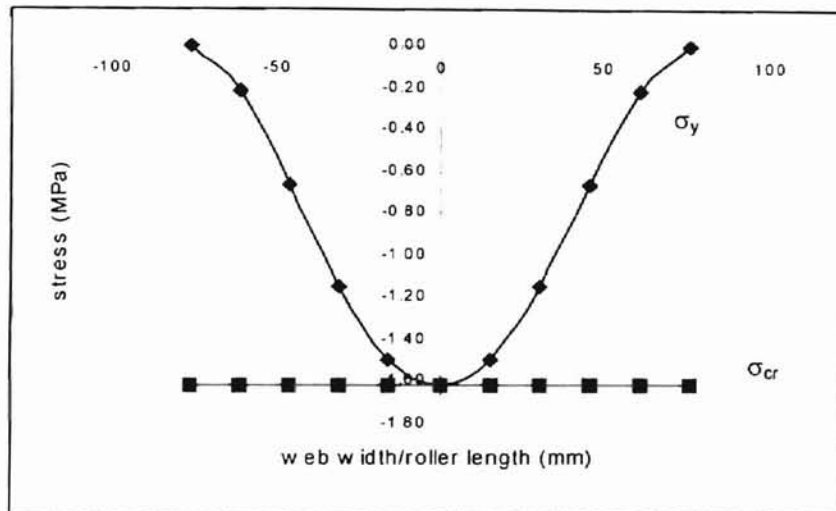


Figure 19. Theoretical stress wrinkling condition. Lateral compressive stress due to web traction σ_y vs. Critical buckling stress σ_{cr}

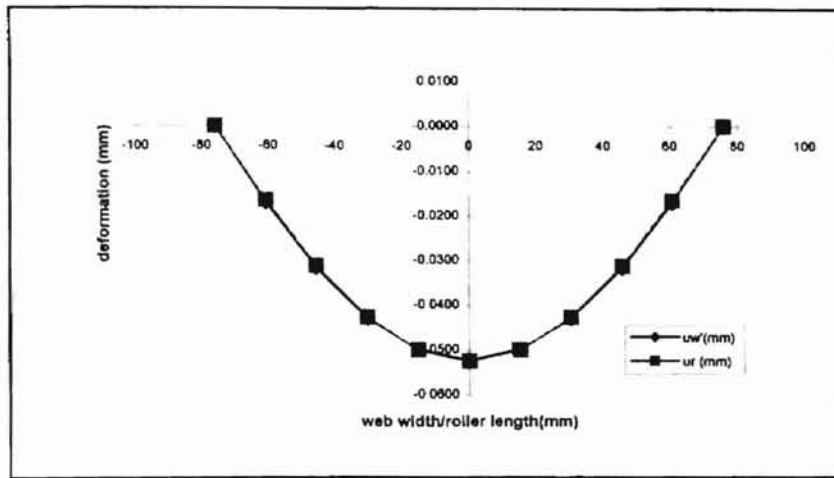


Figure 20. Theoretical compatibility wrinkling condition. Web deformation u_w vs. roller deflection u_r .

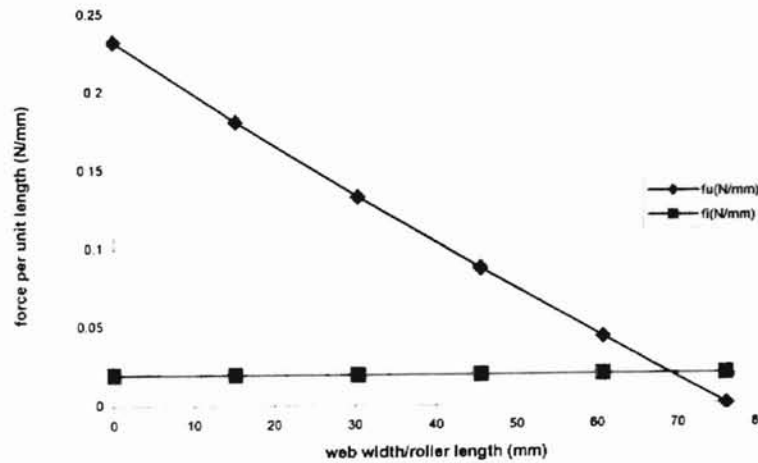


Figure 21. Theoretical frictional wrinkling condition. Lateral surface force f_u vs. lateral internal force f_i .

Similar theoretical computations and graphs were done for each roller size and web caliper at fixed spans and velocities. For all calculations the following were noted :

- 1) The frictional wrinkling condition is overly satisfied when the maximum compressive internal stress σ_y (at the roller center) is equal to the critical buckling stress σ_{cr} , and web deformation at the contact line is very close to roller deflection. Therefore, meeting the stress and compatibility wrinkling conditions, the frictional condition was automatically satisfied.
- 2) For each roller size, web span, and web caliper, the results for wrinkling conditions did not vary for the velocities used in the experiments.

5.2 Comparison between experimental results and initial theoretical computations.

A comparative study between the experimental data and the initial calculations was performed in order to analyze the results and accuracy of the proposed model.

5.2.1 Minimum load R_w required to get web wrinkling.

Figures 22 to 27 compare the experimental minimum load required to get wrinkles $R_w \text{ exp.}$ and the corresponding theoretical value. These are based on the initial computations $R_w \text{ theor.}$ for 31.75 mm (1 ¼ in.) roller, polyester gauge 48 and 38.10 mm (1 ½ in.) roller, polyester gauges 92 and 142. Although the figures below represent only six cases out of thirteen computed and tested in the lab, they describe the pattern observed for all cases.

It was noted that the minimum theoretical wrinkling loads were, always, more than double the experimental values.

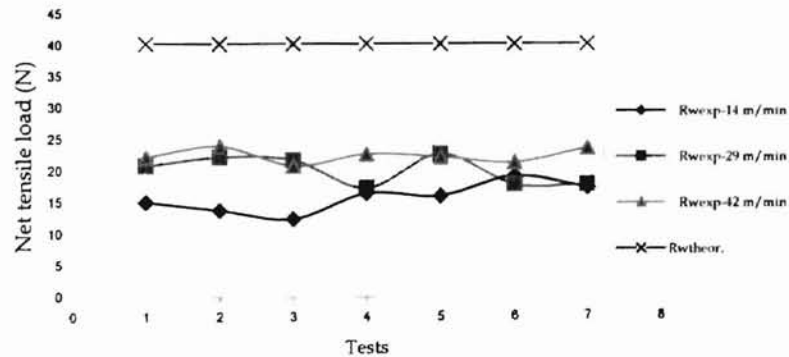


Figure 22. Minimum theoretical load $R_w \text{ theor.}$ according to initial calculations vs. experimental loads $R_w \text{ exp.}$ for 31.75 mm (1 ¼ in.) roller, polyester gauge 48, span = 381 mm at 14, 29 and 42 m/min.

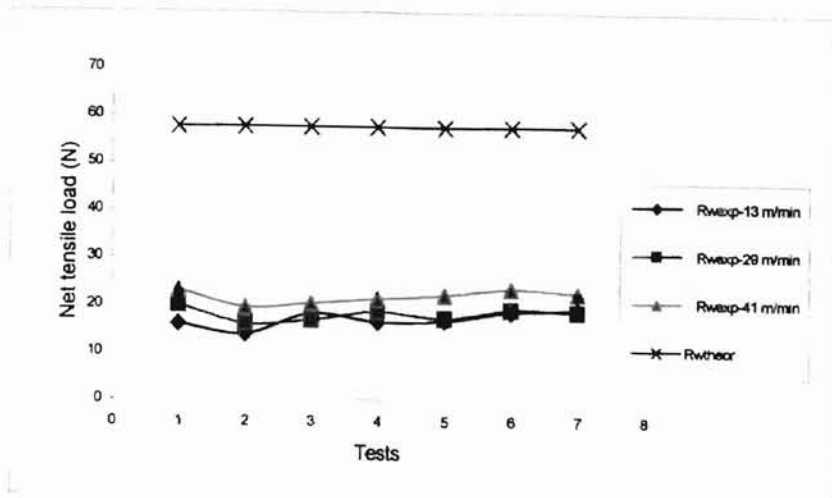


Figure 23. Minimum theoretical load $R_{w,theor}$. according to initial calculations vs. experimental loads $R_{w,exp}$. for 31.75 mm (1 ¼ in.) roller, polyester gauge 48, span = 508 mm at 13, 29 and 41 m/min.

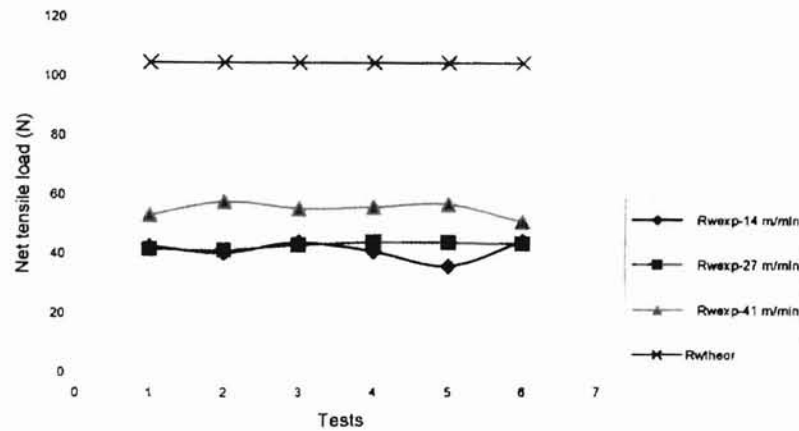


Figure 24. Minimum theoretical load $R_{w,theor}$. according to initial calculations vs. experimental loads $R_{w,exp}$. for 38.10 mm (1 ½ in.) roller, polyester gauge 92, span = 381 mm at 14, 27 and 41 m/min.

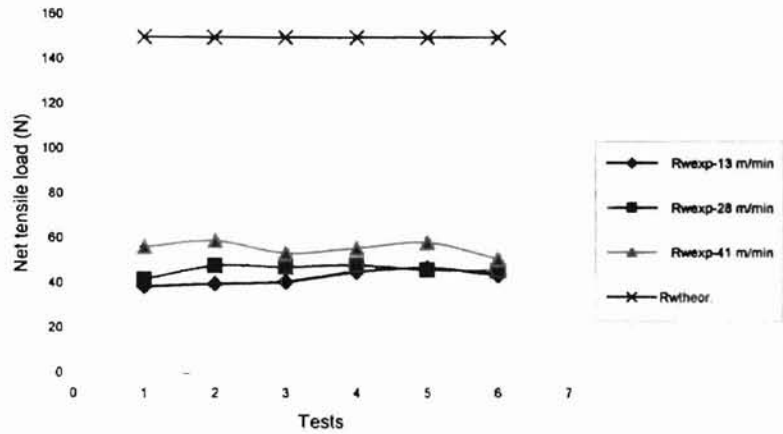


Figure 25. Minimum theoretical load $R_{w,theor}$. according to initial calculations vs. experimental loads $R_{w,exp}$. for 38.10 mm (1 1/2 in.) roller, polyester gauge 92, span = 508 mm at 13, 28 and 41 m/min.

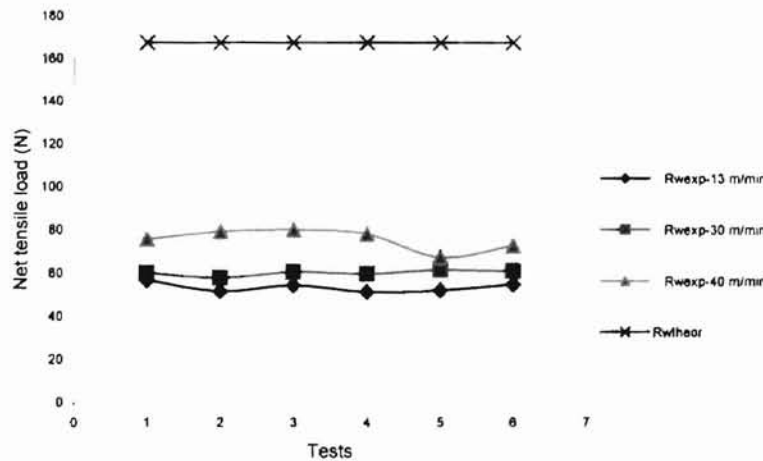


Figure 26. Minimum theoretical load $R_{w,theor}$. according to initial calculations vs. experimental loads $R_{w,exp}$. for 38.10 mm (1 1/2 in.) roller, polyester gauge 142, span = 381 mm at 13, 30 and 40 m/min.

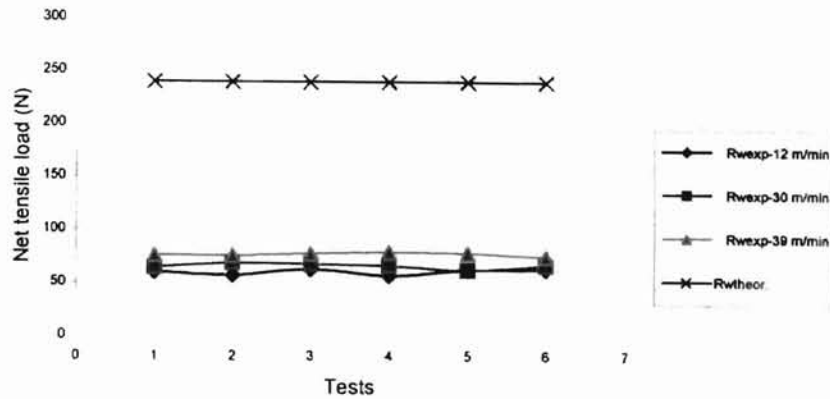


Figure 27. Minimum theoretical load $R_{w,theor}$. according to initial calculations vs. experimental loads $R_{w,exp}$. for 38.10 mm (1 1/2 in.) roller, polyester gauge 142, span = 508 mm at 12, 30 and 39 m/min.

5.2.2 Roller deflection at the center $u_{r-center}$ under wrinkling conditions.

Figures 28 to 32 exhibit the comparison between theoretical roller center deflections according to initial computations and the experimental relative deflections obtained in WHRC for the same cases mentioned in 5.2.1.

For all cases displayed, the theoretical roller center deflections were very high when compared with the experimental relative roller deflections at the center. The deviations between theoretical and experimental values were in the range from 2 to 4.

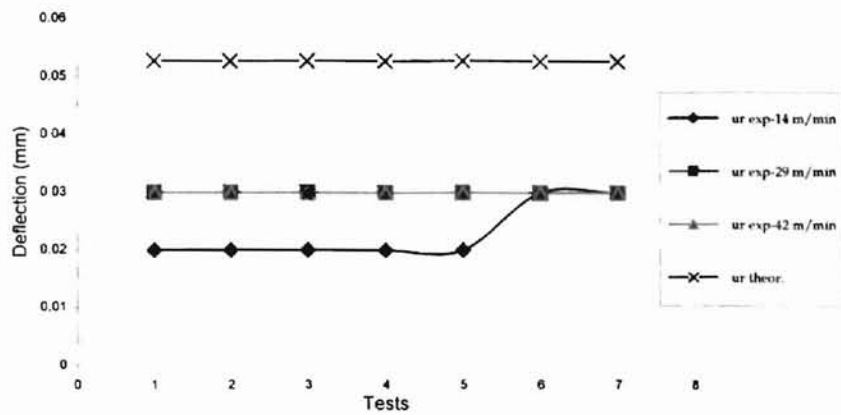


Figure 28. Theoretical roller center deflection $u_{r-theor}$ according to initial computations vs. experimental relative deflections u_{r-exp} for 31.75 mm (1 1/4 in.) roller, polyester gauge 48, span = 381 mm at 14, 29 and 42 m/min.

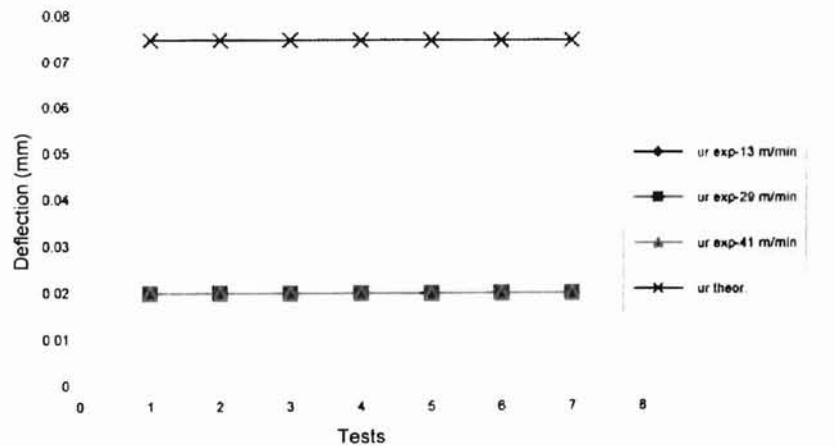


Figure 29. Theoretical roller center deflection $u_{r-theor}$ according to initial computations vs. experimental relative deflections u_{r-exp} for 31.75 mm (1 1/4 in.) roller, polyester gauge 48, span = 508 mm at 13, 29 and 40 fpm.

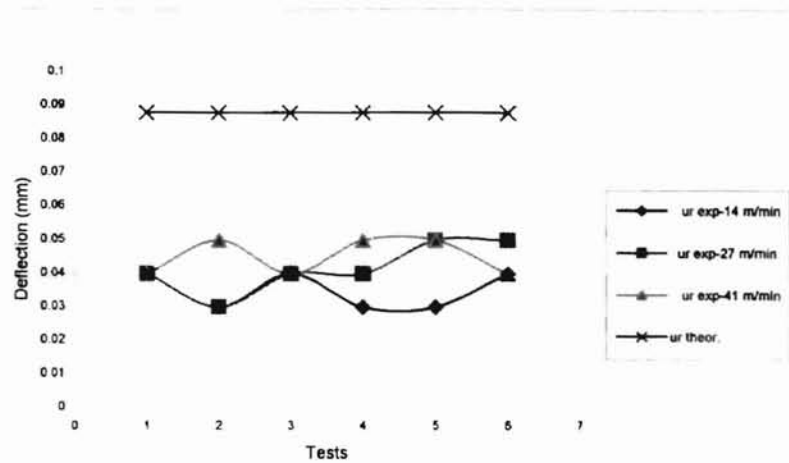


Figure 30. Theoretical roller center deflection $u_{r-theor}$ according to initial computations vs. experimental relative deflections u_{r-exp} for 38.10 mm (1 1/2 in.) roller, polyester gauge 92, span = 381 mm at 14, 27 and 41 m/min.

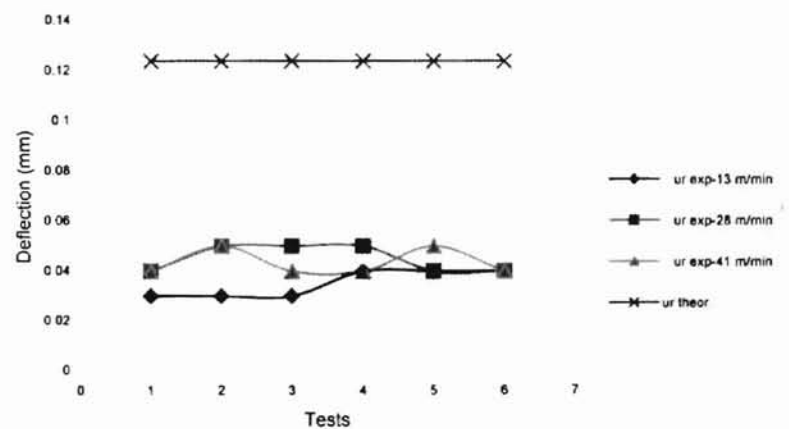


Figure 31. Theoretical roller center deflection $u_{r-theor}$ according to initial computations vs. experimental relative deflection u_{r-exp} for 38.10 mm (1 1/2 in.) roller, polyester gauge 92, span = 508 mm at 13, 28 and 41 m/min.

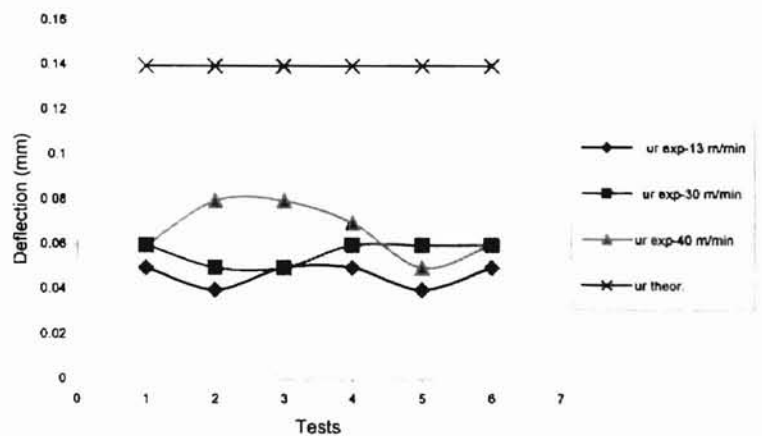


Figure 32. Theoretical roller center deflection $u_{r-theor}$ according to initial computations vs. experimental relative deflections u_{r-exp} for 38.10 mm (1 1/2 in.) roller, polyester gauge 142, span = 381 mm at 13, 30 and 40 m/min .

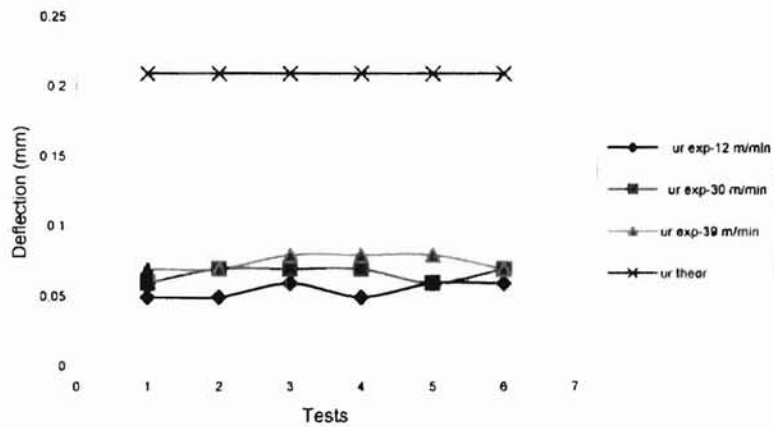


Figure 33. Theoretical roller center deflection $u_{r-theor}$ according to initial computations vs. experimental relative deflections u_{r-exp} for 38.10 mm (1 1/2 in.) roller, polyester gauge 142, span = 508 mm at 12, 30 and 39 m/min.

5.2.3 Discussion

The comparison between the theoretical loads and deflections, based on the initial computations, and the experimental values obtained in the lab did not match. These differences make the predictions unacceptable.

Three (3) important factors may be observed :

- a- A large difference between the minimum wrinkling theoretical loads $R_w theor.$ and the experimental values $R_w exp.$. The theoretical loads were very high compared with the experimental ones, in some cases the predicted load would be impossible to reach at the testing machine, but , during the corresponding experiments, we acquired wrinkles under less loading conditions.
- b- Very high theoretical roller deflections at the center $u_{r-theor}$ compared with the experimental relative deflections u_{r-exp} . This notable theoretical-experimental deviation for the roller deflection can be interpreted as follows: the roller should be subjected to a load greater than the minimum required to wrinkle the web in order to meet the theoretical stress and compatibility wrinkling conditions.
- c- The large high values for the lateral surface force $f\mu$ at the roller center, with respect to the internal forces f_i , seem to support the inference about an excessive computed load. A high $R_w theor.$ implies

high $S1$ and $S2$ that increase the value of $f\mu$ according to equation [35].

In order to analyze in detail our hypothesis, we computed the internal web stress in CMD σ_y (equation [15]) and the roller center deformation $u_{r-center}$ (equation [31]) using the experimental loads obtained during the tests .

Figures 34 to 39 show the comparison between the internal web stress with the roller under the experimental loads, and the respective critical buckling stress for roller sizes 31.75 mm (1 ¼ in.) and 38.10 mm (1 ½ in.) and web thickness of gauge 48, 92 and 142 as follows:

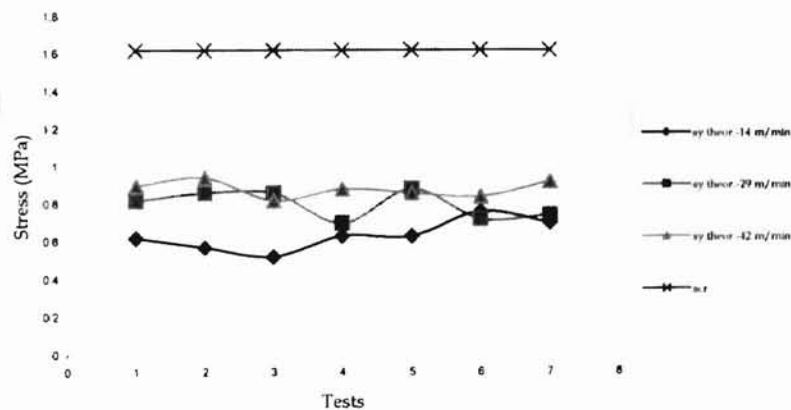


Figure 34. Theoretical internal stress in CMD σ_y vs. critical buckling stress σ_{cr} at experimental net forces R_w exp. for 31.75 mm (1 ¼ in.) roller, polyester gauge 48 and span = 381 mm.

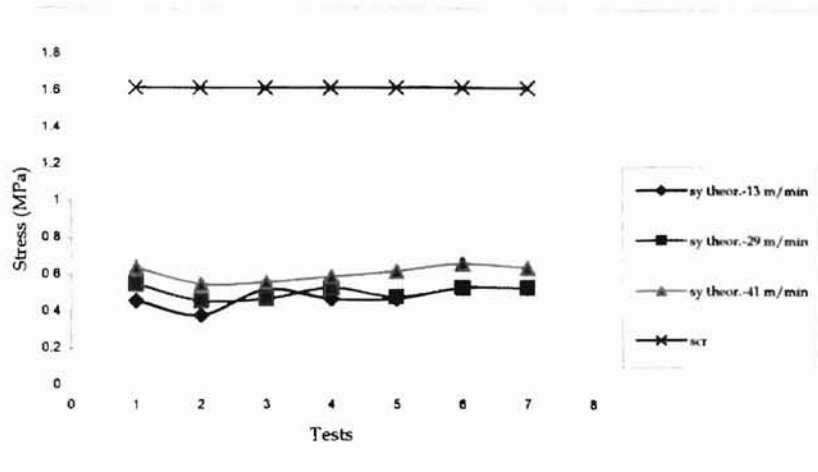


Figure 35. Theoretical internal stress in CMD σ_y vs. critical buckling stress σ_{cr} at experimental net forces R_w exp. for 31.75 mm (1 ¼ in.) roller, polyester gauge 48 and span= 508 mm.

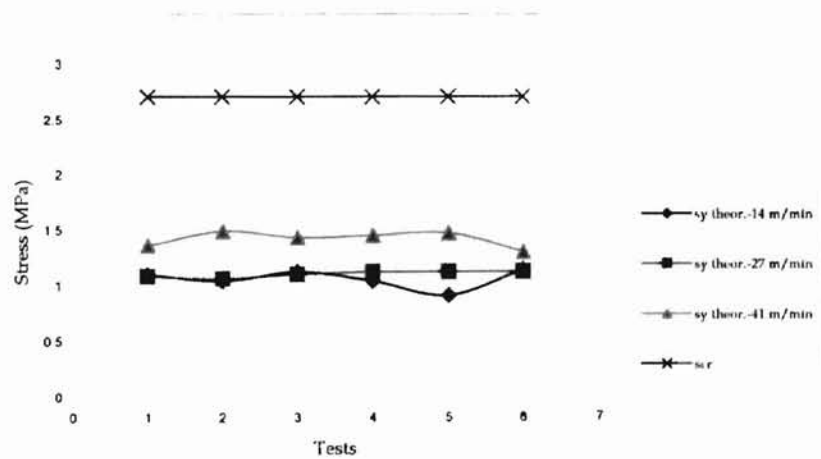


Figure 36. Theoretical internal stress in CMD σ_y vs. critical buckling stress σ_{cr} at experimental net forces R_w exp. for 38.10 mm (1 ½ in.) roller, polyester gauge 92 and span = 381 mm.

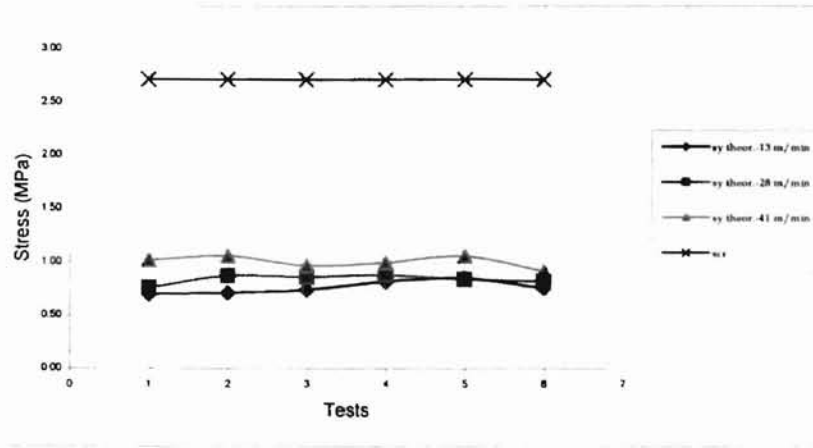


Figure 37. Theoretical internal stress in CMD σ_y vs. critical buckling stress σ_{cr} at experimental net forces R_w exp. for 38.10 mm (1 1/2 in.) roller, Polyester gauge 92 and span= 508 mm.

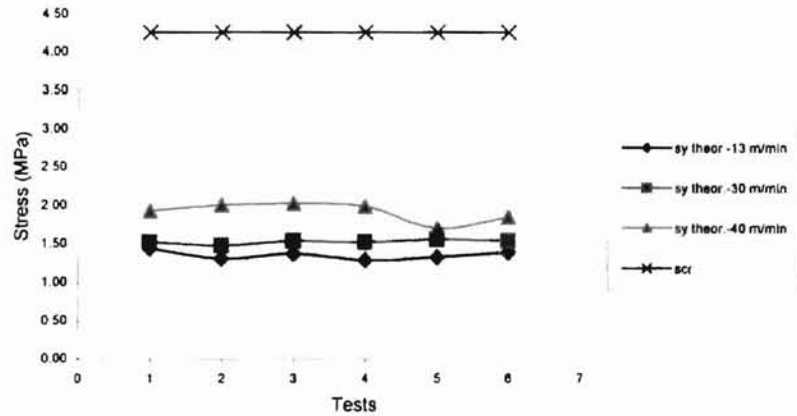


Figure 38. Theoretical internal stress in CMD σ_y vs. critical buckling stress σ_{cr} at experimental net forces R_w exp. for 38.10 mm (1 1/2 in.) roller, Polyester gauge 142 and span= 381 mm.

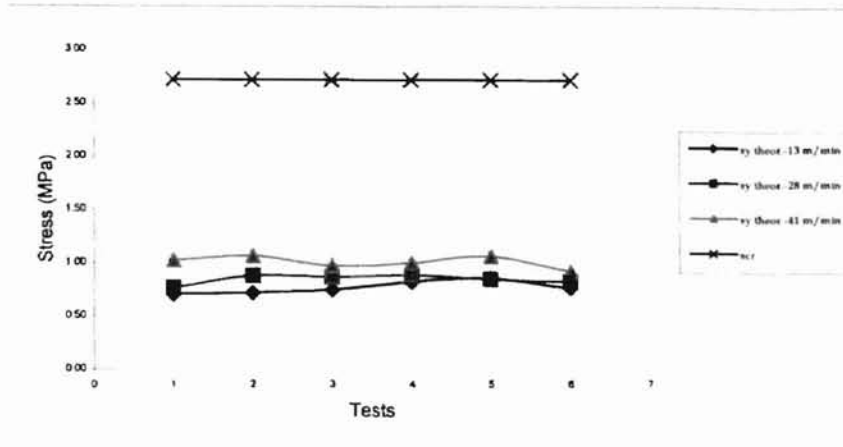


Figure 37. Theoretical internal stress in CMD σ_y vs. critical buckling stress σ_{cr} at experimental net forces R_w exp. for 38.10 mm (1 1/2 in.) roller, Polyester gauge 92 and span= 508 mm.

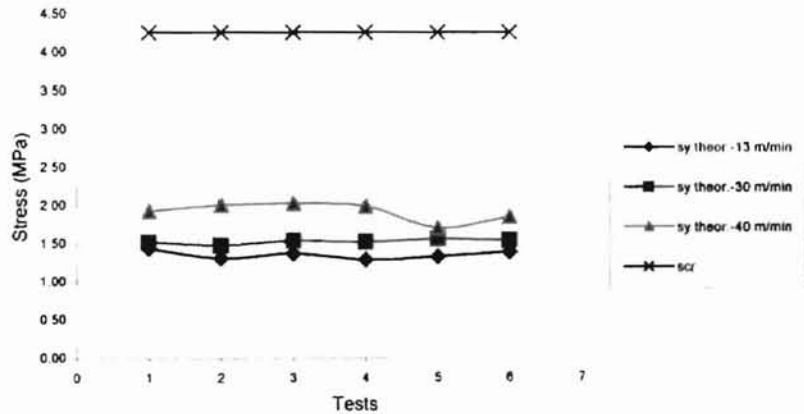


Figure 38. Theoretical internal stress in CMD σ_y vs. critical buckling stress σ_{cr} at experimental net forces R_w exp. for 38.10 mm (1 1/2 in.) roller, Polyester gauge 142 and span= 381 mm.

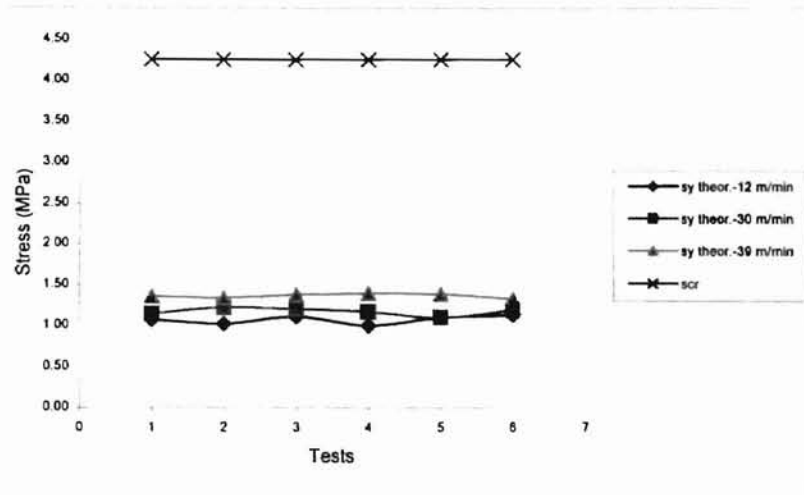


Figure 39. Theoretical internal stress in CMD σ_y vs. critical buckling stress σ_{cr} at experimental net forces R_w exp. for 38.10 mm (1 1/2 in.) roller, polyester gauge 142 and span = 508 mm.

As can be seen from figures 34 to 39, the internal web stress σ_y is not large enough, itself, to produce simultaneously stress, compatibility, and frictional wrinkling conditions. For that reason, the iterative predictive computation on our spreadsheet needed to assume a greater load (than the minimum required for wrinkling) to achieve the simultaneous presence of the three mentioned wrinkling conditions.

The theoretical roller center deflections with the roller under the experimental loads, and the experimental relative deflections are compared in Figures 40 to 45.

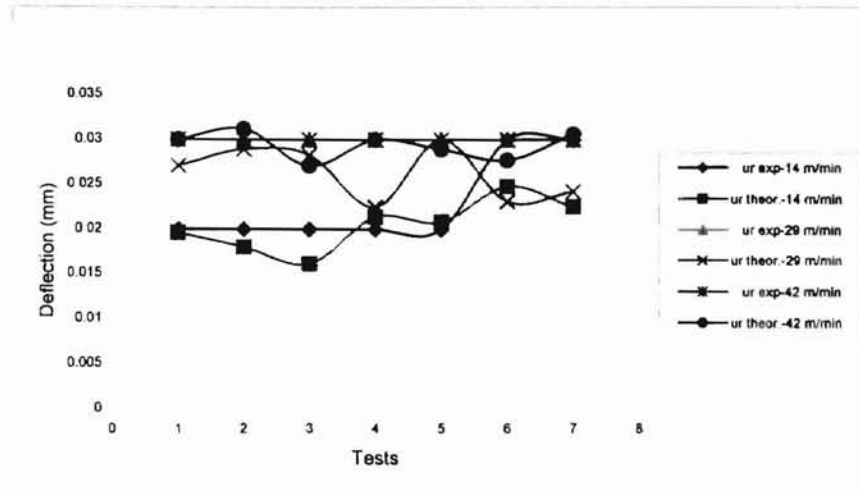


Figure 40. Theoretical ($u_r, theor.$) vs. experimental ($u_r, exp.$) roller center deflections at experimental loads $R_w exp.$ for 31.75 mm ($1 \frac{1}{4}$ in.) roller, polyester gauge 48 and span = 381 mm at 14 , 29 and 42 m/min.

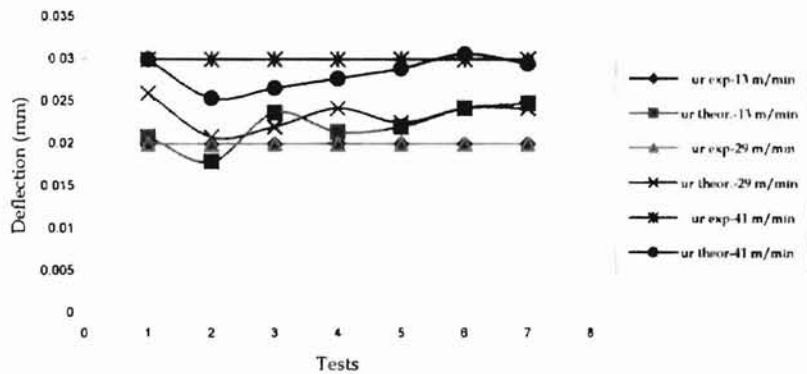


Figure 41. Theoretical ($u_r, theor.$) vs. experimental ($u_r, exp.$) roller center deflections at experimental loads $R_w exp.$ for 31.75 mm ($1 \frac{1}{4}$ in.) roller, polyester gauge 48 and span = 508 mm at 13, 29 and 41 m/min.

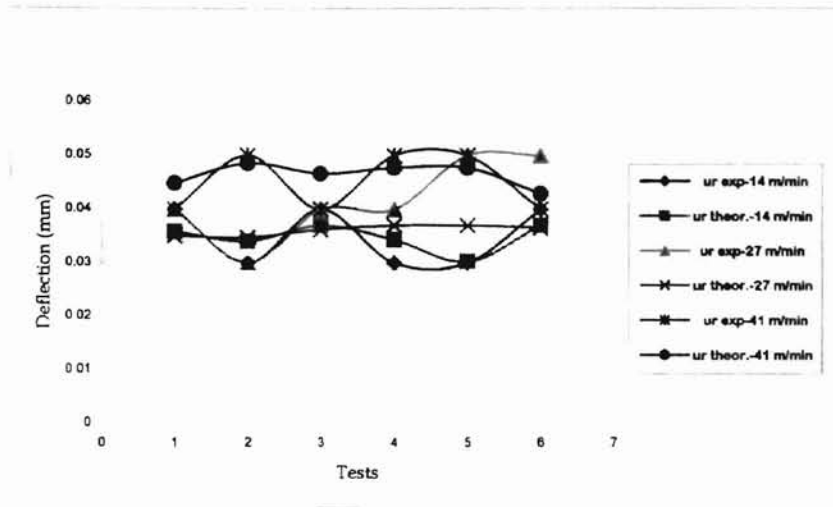


Figure 42. Theoretical ($u_r, theor.$) vs. experimental ($u_r, exp.$) roller center deflections at experimental loads $R_w, exp.$ for 38.10 mm (1 1/2 in.) roller, polyester gauge 92 and span = 381 mm at 14, 27 and 41 m/min.

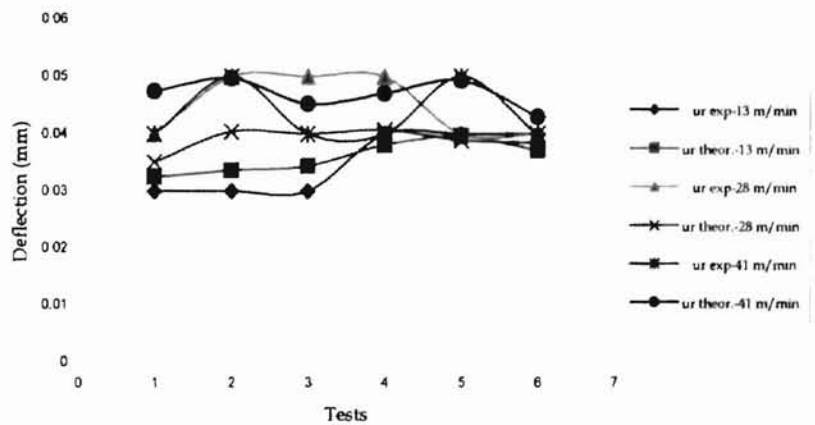


Figure 43. Theoretical ($u_r, theor.$) vs. experimental ($u_r, exp.$) roller center deflections at experimental loads $R_w, exp.$ for 38.10 mm (1 1/2 in.) roller, polyester gauge 92 and span = 508 mm at 13, 28 and 41 m/min.

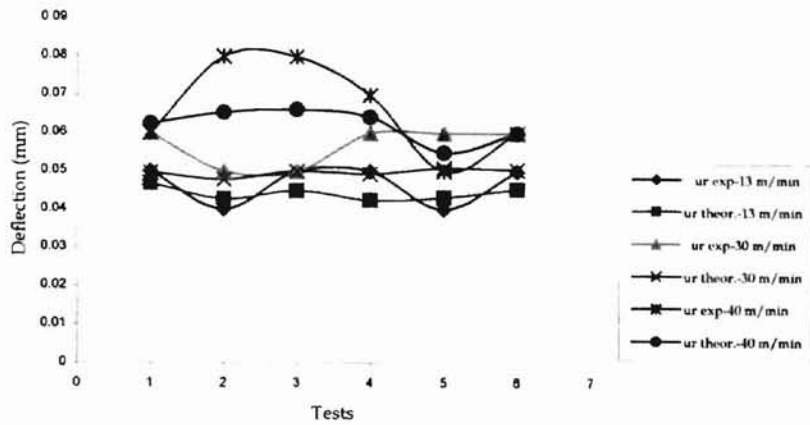


Figure 44. Theoretical ($u_r, theor.$) vs. experimental ($u_r, exp.$) roller center deflections at experimental loads $R_w, exp.$ for 38.10 mm (1 1/2 in.) roller, polyester gauge 142 and span = 15 inches at 13, 30 and 40 m/min.

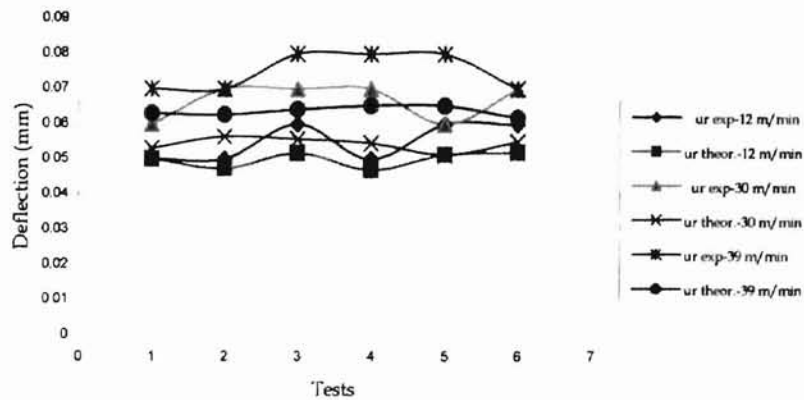


Figure 45. Theoretical ($u_r, theor.$) vs. experimental ($u_r, exp.$) roller center deflections at experimental loads $R_w, exp.$ for 38.10 mm (1 1/2 in.) roller, polyester gauge 142 and span = 508 mm at 12, 30 and 39 m/min.

From Figures 40 to 45, we can observe that under the experimental loads, the proposed method gives us an acceptable correlation between theoretical and experimental roller deflections at its center. Now, the problem is focused on correcting the necessary stress that satisfies the stress wrinkling condition and correlates with the experimental data.

5.3 Modified Stress Wrinkling Condition.

Duvall (6) found, in his experimental research, that the theoretical roller bending strain matched better than Shelton's proposed strain (strain caused by steering of the deflected roller) for his particular model.

In our case, we can not simply substitute the internal web stress in CMD, σ_y , by the roller bending stress because of the likeness between theoretical and experimental roller center deflections shown in figures 40 to 45.

The theoretical roller deflection u_r (equation [31]) is a function of roller properties and dimensions, web thickness and the numerical coefficients $S1$ and $S2$ of the parabolic web traction q . This web traction is responsible, at the same time, for the roller deflection and the web deformation. Therefore our assumption is based on the web is subjected simultaneously to the internal stress

σ_y that is stretching it, plus the roller bending stress σ_b that is imparted to the web in contact with the roller, so that the web can assume the same roller shape.

The maximum compressive stress due to roller bending is located on the top surface of the roller and contributes, with the internal web stress, to surpass the critical stress for buckling.

Now, the stress wrinkling condition becomes:

$$\sigma_{ly} \geq \sigma_{cr} \quad [42]$$

where σ_{ly} is the total stress in the cross machine direction and is given by the following expression:

$$\sigma_{ly} = \sigma_y + \sigma_b \quad [43]$$

where σ_y is the internal web stress in CMD (equation [15]) and σ_b is the maximum bending roller stress.

The expression for the maximum compressive stress on the roller surface due to bending is:

$$\sigma_b = E_{w-CMD} (R + t_w) \frac{d^2 u_r}{dy^2} \quad [44]$$

where E_{w-CMD} is the modulus of elasticity in the cross machine direction.

In the development of this study, we have considered the web as an isotropic material; accepting that this assumption is not rigorously true, we can assume:

$$E_{w-CMD} \cong E_{w-MD} \quad [45]$$

New computations based on the modified stress wrinkling conditions (equation [42]) in the proposed method were done to find the minimum theoretical loads to achieve wrinkles and the roller center deflections. These theoretical values are compared with the experimental ones in figures 46 to 57 as follows:

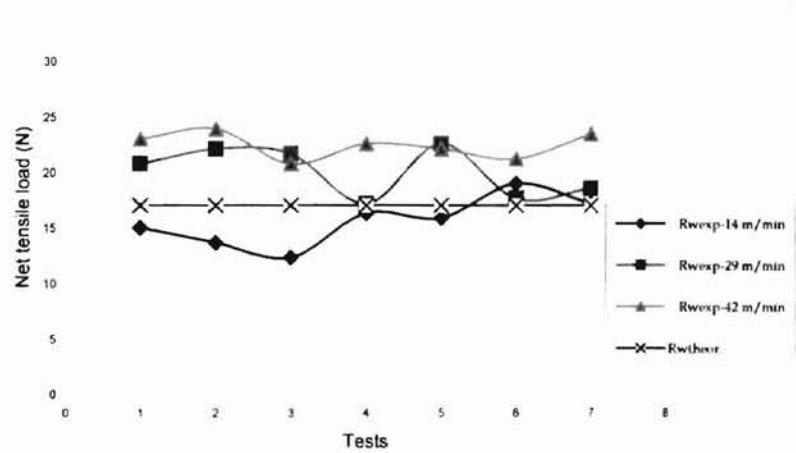


Figure 46. Minimum theoretical load $R_{w,theor}$. considering total stress in CMD σ_{iy} vs. experimental loads $R_{w,exp}$. for 31.75 mm (1 1/4 in.) roller, polyester gauge 48, span = 381 mm at 14, 29 and 42 m/min.

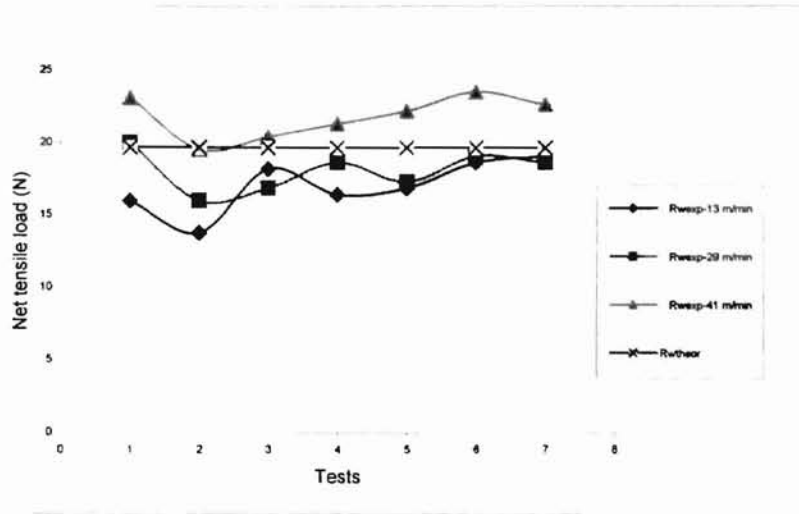


Figure 47. Minimum theoretical load $R_w theor.$ considering total stress in CMD σ_y vs. experimental loads $R_w exp.$ for 31.75 mm (1 ¼ in.) roller, polyester gauge 48, span = 508 mm at 13, 29 and 41 m/min.

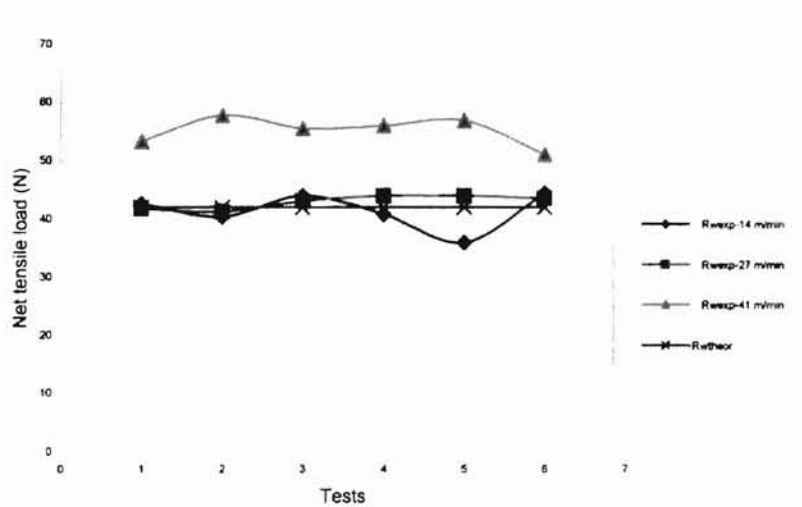


Figure 48. Minimum theoretical load $R_w theor.$ considering total stress in CMD σ_y vs. experimental loads $R_w exp.$ for 38.10 mm (1 ½ in.) roller, polyester gauge 92, span = 381 mm at 14, 27 and 41 m/min.

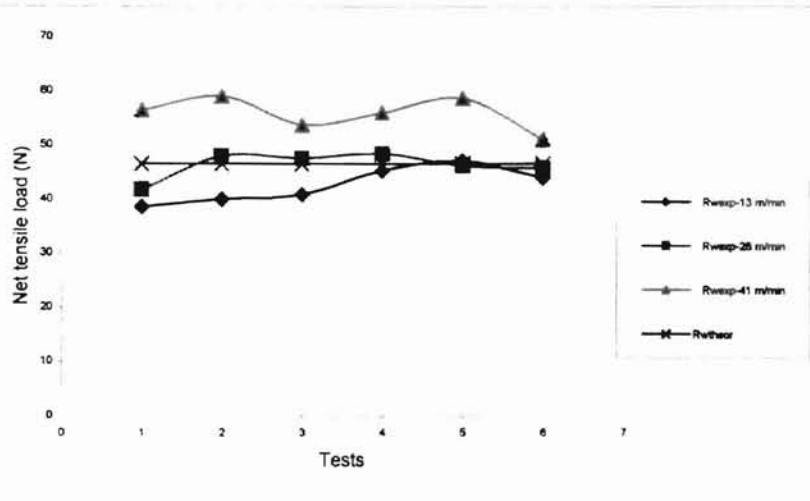


Figure 49. Minimum theoretical load $R_w theor.$ considering total stress in CMD σ_{iy} vs. experimental loads $R_w exp.$ for 38.10 mm (1 1/2 in.) roller, polyester gauge 92, span = 508 mm at 13, 28 and 41 m/min.

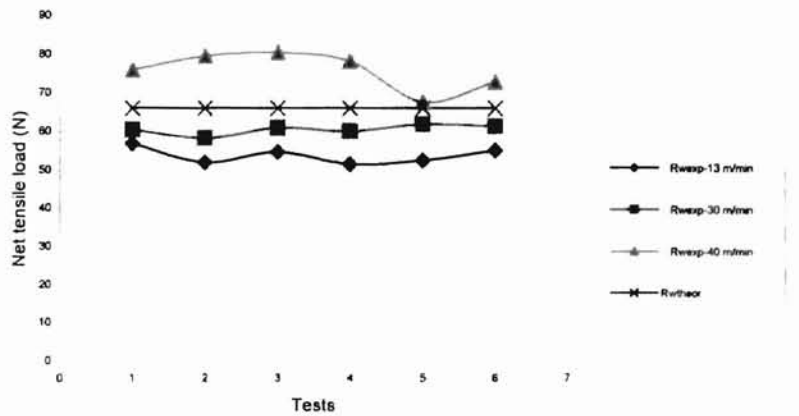


Figure 50. Minimum theoretical load $R_w theor.$ considering total stress in CMD σ_{iy} vs. experimental loads $R_w exp.$ for 38.10 mm (1 1/2 in.) roller, polyester gauge 142, span = 381 mm at 13, 30 and 40 m/min.

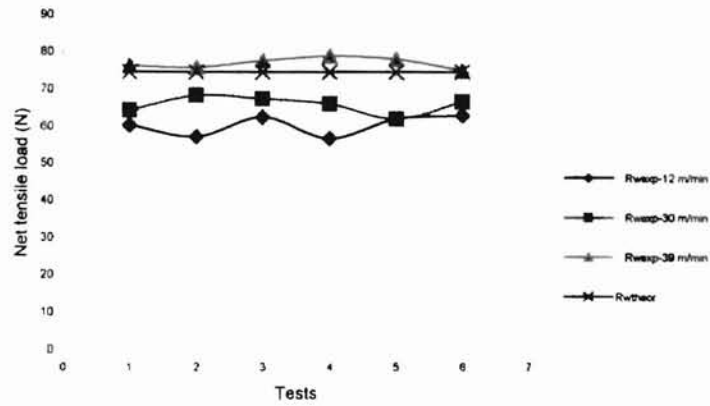


Figure 51. Minimum theoretical load $R_{w,theor}$. considering total stress in CMD σ_y vs. experimental loads $R_{w,exp}$. for 38.10 mm (1 1/2 in.) roller, polyester gauge 142, span = 508 mm at 12, 30 and 39 m/min.

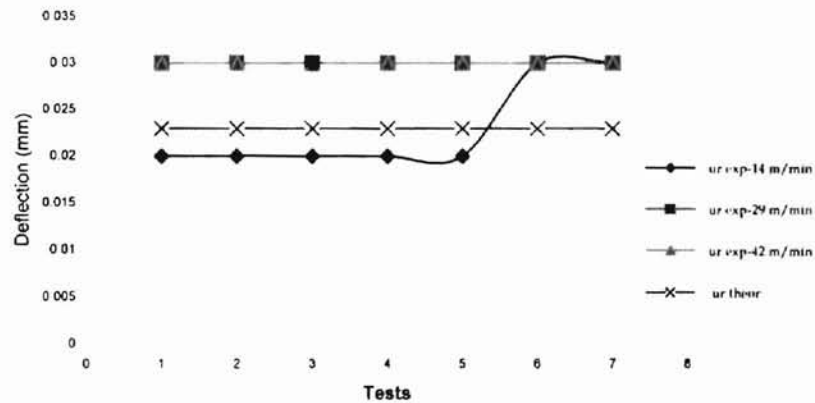


Figure 52. Theoretical ($u_{r,theor}$) vs. experimental ($u_{r,exp}$) roller center deflections considering total stress in CMD σ_y for 31.75 mm (1 1/4 in.) roller, polyester gauge 48 and span = 381 mm at 14, 29 and 42 m/min.

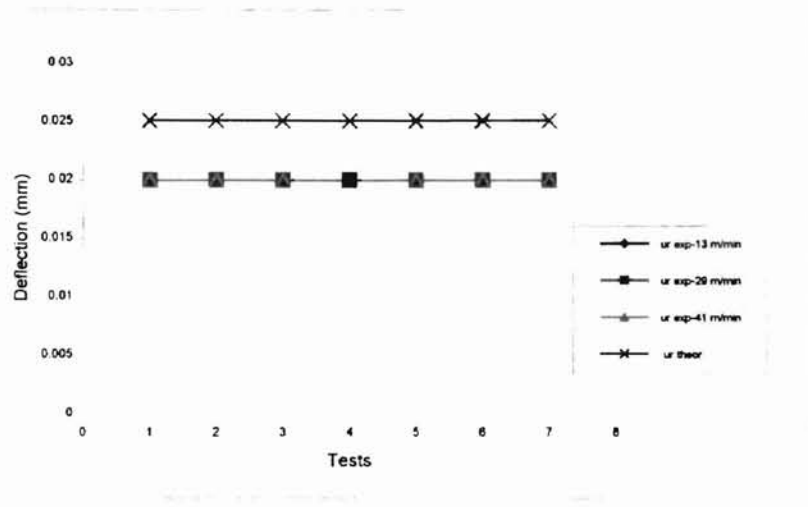


Figure 53. Theoretical ($u_r theor.$) vs. experimental ($u_r exp.$) roller center deflections considering total stress in CMD σ_y for 31.75 mm (1 ¼ in.) roller, polyester gauge 48 and span = 508 mm at 13, 29 and 41 m/min.

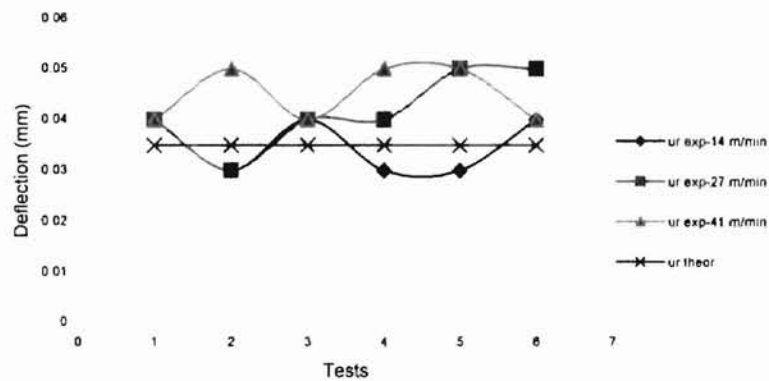


Figure 54. Theoretical ($u_r theor.$) vs. experimental ($u_r exp.$) roller center deflections considering total stress in CMD σ_y for 38.10 mm (1 ½ in.) roller, polyester gauge 92 and span = 381 mm at 14, 27 and 41 m/min.

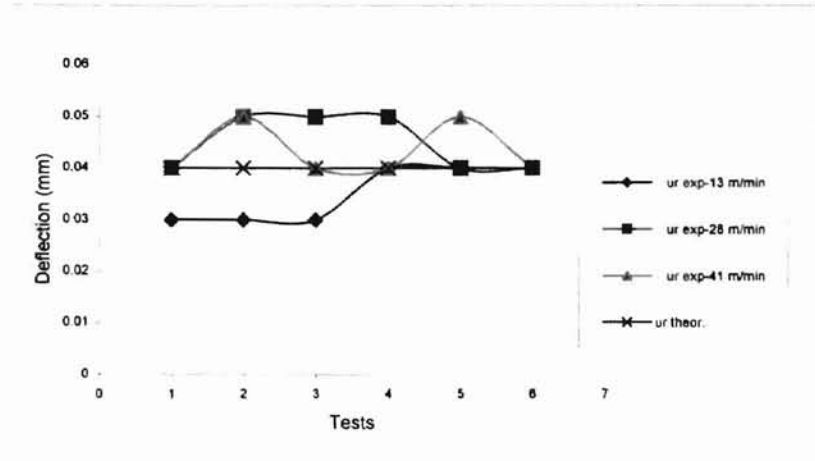


Figure 55. Theoretical ($u_r, theor.$) vs. experimental ($u_r, exp.$) roller center deflections considering total stress in CMD σ_{ty} for 38.10 mm (1 1/2 in.) roller, polyester gauge 92 and span = 508 mm at 13, 28 and 41 m/min.

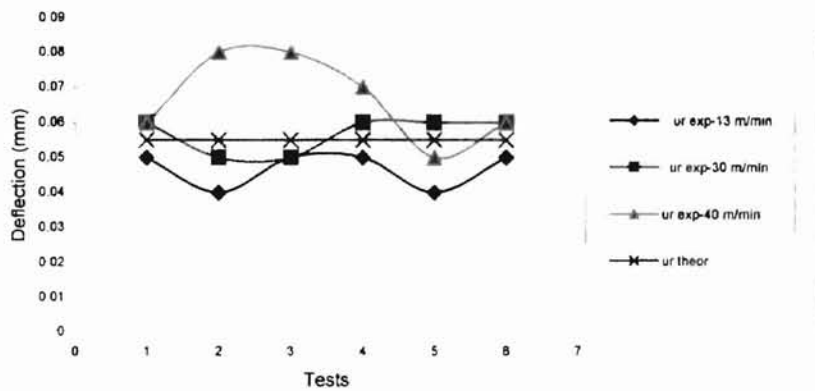


Figure 56. Theoretical ($u_r, theor.$) vs. experimental ($u_r, exp.$) roller center deflections considering total stress in CMD σ_{ty} for 38.10 mm (1 1/2 in.) roller, polyester gauge 142 and span = 381 mm at 13, 30 and 40 m/min.

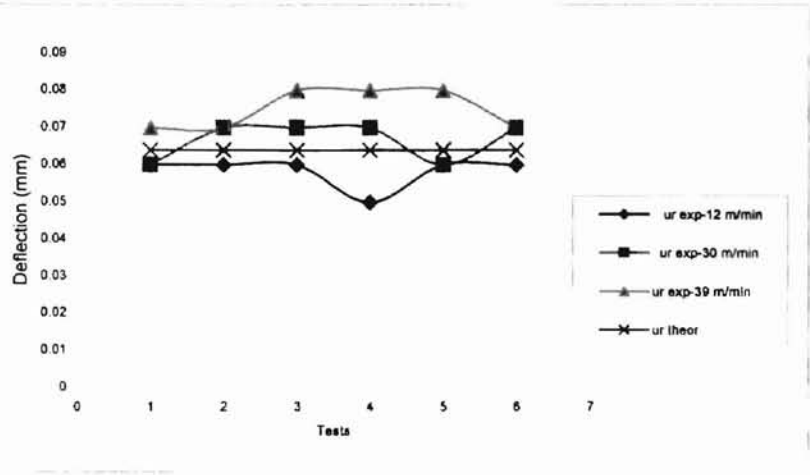


Figure 57. Theoretical ($u_r, theor.$) vs. experimental ($u_r, exp.$) roller center deflections considering total stress in CMD σ_y for 38.10 mm (1 1/2 in.) roller, polyester gauge 142 and span = 508 mm at 12, 30 and 39m/min.

Table 5 shows the comparison between the theoretical wrinkling loads and the mean values for the experimental wrinkling loads obtained from the testing machine. The standard deviations for the experimental values are also indicated.

Case	Description	Mean values for R_w exp		Stand. dev. of R_w exp
		R_w theor. (Newtons)	R_w exp. (Newtons)	SD R_w exp. (Newtons)
1	Roller: 31.75 mm, Web: gauge 48, span:381 mm.	17.17	19.51	0.77
2	Roller: 31.75 mm, Web: gauge 48, span:508 mm.	19.70	19.00	0.58
3	Roller: 31.75 mm, Web: gauge92, span:381 mm.	34.38	37.26	1.69
4	Roller: 31.75 mm, Web: gauge 92, span:508 mm.	39.05	39.57	1.03
5	Roller: 31.75 mm, Web: gauge 142, span:381 mm.	55.29	56.61	1.84
6	Roller: 31.75 mm, Web: gauge 142, span:508 mm.	62.76	71.04	2.56
7	Roller: 38.10 mm, Web: gauge 48, span:381 mm.	21.13	23.80	0.80
8	Roller: 38.10 mm, Web: gauge 48, span:508 mm.	23.93	23.62	0.73
9	Roller: 38.10 mm, Web: gauge 92, span:381 mm.	42.08	46.53	1.51
10	Roller: 38.10 mm, Web: gauge 92, span:508 mm.	46.62	48.31	1.43
11	Roller: 38.10 mm, Web: gauge 142, span:381 mm.	66.05	63.38	2.23
12	Roller: 38.10 mm, Web: gauge 142, span:508 mm.	74.82	67.88	1.67
13	Roller: 58.10 mm, Web: gauge 48, span:381 mm.	90.29	94.74	0.98

As can be seen in the figures 46 to 57 and Table 5, the assumption that the web is bearing simultaneously the internal stress in CMD and the bending stress, agrees more closely with the experimental results. This gives a better relationship between the theoretical wrinkling loads and roller center deflections and the experimental ones.

Figures 58 to 60 show how the frictional wrinkling condition is satisfied for the cases studied. No relevant change in the lateral surface force f_{μ} was observed at the different tested velocities for each roller.

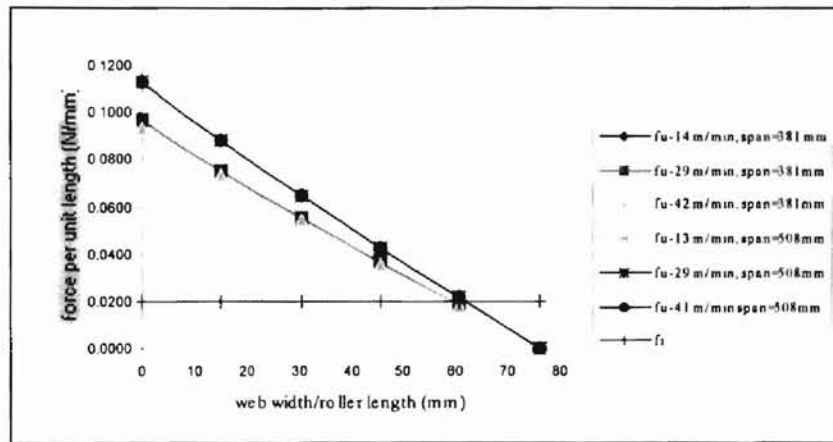


Figure 58. Lateral surface force f_{μ} vs. internal force f_i , considering σ_{ty} for 31.75 mm (1 1/4 in.) roller and polyester gauge 48 at the tested velocities.

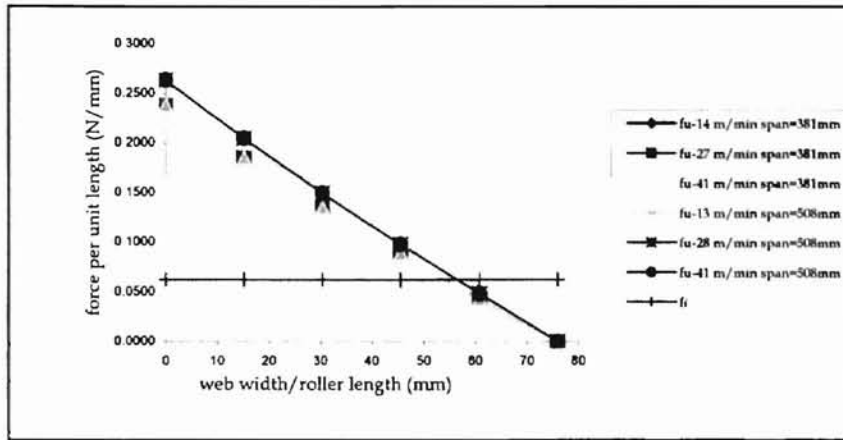


Figure 59. Lateral surface force f_{μ} vs. internal force f_i considering σ_{ty} for 38.10 mm (1 1/2 in.) roller and polyester gauge 92 at the tested velocities.

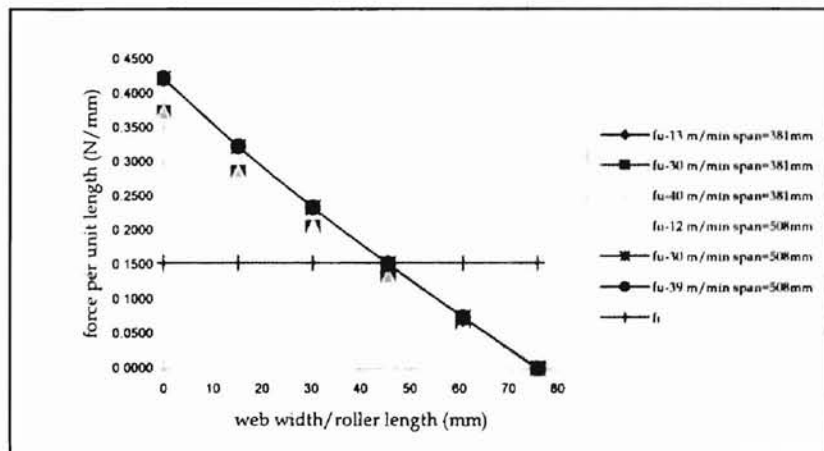


Figure 60. Lateral surface force f_{μ} vs. internal force f_i considering σ_{ty} for 38.10 mm (1 1/2 in.) roller and polyester gauge 142 at the tested velocities.

CHAPTER 6

CONCLUSIONS AND RECOMMENDATIONS

The intent of this study was to develop a practical model to predict web wrinkling due to roller deflection based on the theory of elasticity, by using Shelton's theory and previous works in this area. The result was a theoretical procedure that allows an acceptable accuracy within the experimental data. Some of the important conclusions that were drawn from the theoretical and experimental work described above are given below.

1. A parabolic web traction in the machine direction is responsible for the roller deflection and web deformation in the same direction. When this traction reaches a critical value, wrinkles start appearing within the web wrapping the deflected roller.
2. The minimum parabolic web traction that produces web wrinkling over the roller is unique and its distribution along the web width is governed by two (2) numerical coefficients developed in this study ($S1$ & $S2$).
3. As a consequence of that parabolic web traction, three (3) simultaneous conditions are required to be present for web wrinkles over a deflected roller, they are:

- The maximum total web stress in the cross machine direction should be greater or equal than the critical buckling stress for a cylindrical web shell without internal pressure. This maximum total stress is the result of the maximum internal web stress due to the parabolic web traction, and the maximum roller stress due to bending .
- The web must assume the shape of the deflected roller. For this reason, at the contact area, the web deformation in the machine direction should match with the roller deflection.
- The frictional force between web and roller should be greater than the internal force due to web buckling. This frictional force is affected by the coefficient of friction web-roller and by the thickness of the air film between web and roller.

The model given above describes the general situation of the wrinkling of webs due to roller curvature. Further studies should consider additional web and roller sizes and materials, spans, and velocities that can have a major effect on the web lateral slippage over the roller.

Since most webs are not isotropic materials, the effect of web anisotropy on the web wrinkles due to roller curvature should also be investigated in future studies.

REFERENCES

1. Good, J. K. and Delahoussaye, R. D., "Analysis of Web Spreading Induced by The Concave Roller ", Proceedings of the Second International Conference on Web Handling, June 6-9, 1993, Oklahoma State University, Stillwater, OK.
2. Hakiel, Z., "From predictive Models to Profitability in The Web-Handling Industry", Proceedings of the Third International Conference on Web Handling, June 18-21, 1995, Oklahoma State University, Stillwater, OK.
3. Good, J. K., Gehlbach, L. S. and Kedl, D. M., "Predicting Shear Wrinkles in Web Spans", TAPPI Journal, August, 1989.
4. Shelton, J. J., "Machine Direction Troughs in Web Spans and Corrugations in Wound Rolls", Web Handling Research Center Oklahoma State University, August, 1991.
5. Timoshenko, S. P. and Gere, J. M., "Theory of Elastic Stability" McGraw-Hill Book Company, New York, Second Edition, 1961.
6. Duvall, M. G. " A Study of Web Wrinkling Due to Roller Curvature", Thesis, Department of Mechanical and Aerospace Engineering, Oklahoma State University, 1997.
7. Ugural, A. C. and Fenster, S. K., "Advanced Strength and Applied Elasticity" Elsevier North Holland Publishing Co., New York, Third Edition, 1975.
8. Rivello, R. M., "Theory and Analysis of Flight Structures", McGraw-Hill Book Company, New York, First Edition, 1969.
9. Good, J. K., Kedl, D. M. and Shelton, J. J., "Shear Wrinkling in Isolated Spans", Proceedings of the Fourth International Conference on Web Handling, June 1-4, 1997, Oklahoma State University, Stillwater, OK.
10. Knox, K. L. and Sweeney, T. L. , "Fluid Effects Associated with Web Handling", Industrial Engineering Chemical Process Design development, Vol. 10, No 2, pp. 201-205.

VITA

Pedro Arias

Candidate for the degree of

Master Science

Thesis: **PREDICTION OF WEB WRINKLING INDUCED BY ROLLER DEFLECTION**

Major Field: Mechanical Engineering

Biographical:

Personal Data: Born in Barcelona , Venezuela, On June 4, 1959, the son of Pedro Arias and Ana Diaz de Arias.

Education: Graduated from T. A. Calatrava High School, Puerto La Cruz, Venezuela in June 1976; received Bachelor of Science degree in Mechanical Engineering from Universidad Central de Venezuela, Caracas, Venezuela in June of 1981. Completed the requirements for the Master of Science degree in Mechanical engineering at Oklahoma State University in July, 1998.

Experience: Mechanical Engineer assigned to Gas Dpt. in Meneven SA, Venezuela from 1981 to 1984, Project Engineer in Polar, Venezuela from 1984 to 1987, Mechanical Engineer in Petroleos de Venezuela, S.A. (PDVSA) from 1987 to 1996, Graduate Research Assistant in the Web Handling Research Center at Oklahoma State University from summer 1997 to present.